

Geophysical Studies to Detect the Acme Underground Coal Mine, Wyoming

U.S. GEOLOGICAL SURVEY BULLETIN 1677



Geophysical Studies to Detect the Acme Underground Coal Mine, Wyoming

By C.H. MILLER

Magnetic, electromagnetic, gravimetric, seismic refraction, and precise topographic surveys gave only subtle hints of underground openings, suggesting the need for further research in geophysical techniques

U.S. GEOLOGICAL SURVEY BULLETIN 1677

DEPARTMENT OF THE INTERIOR
DONALD PAUL HODEL, Secretary



U.S. GEOLOGICAL SURVEY
Dallas L. Peck, Director

UNITED STATES GOVERNMENT PRINTING OFFICE: 1988

For sale by the
Books and Open-File Reports Section
U.S. Geological Survey
Federal Center, Box 25425
Denver, CO 80225

Library of Congress Cataloging in Publication Data

Miller, C. H. (Carter H.)

Geophysical studies to detect the Acme Underground Coal Mine, Wyoming.

(U.S. Geological Survey bulletin ; 1677)

Bibliography: p.

Supt. of Docs. no.: 19.3:1677

1. Acme Underground Coal Mine (Wyo.) 2. Geophysics—Wyoming—
Acme Underground Coal Mine—Methodology. I. Title. II. Series.

QE75.B9 no. 1677

557.3 s

86-600164

[TN805.W8]

[622'334'0978732]

CONTENTS

Abstract	1
Introduction	1
Acknowledgments	2
The Acme Mine	2
Geophysical surveys	6
Site 1	6
Magnetic anomalies caused by heating rocks and by iron	6
Magnetic survey and magnetic field characteristics	7
Site 2	11
Topographic survey	11
Magnetic survey and magnetic field characteristics	11
Electromagnetic survey and electromagnetic field characteristics	13
Gravity survey and gravity field characteristics	15
Seismic survey	20
Soil arch (site 1) as model	22
Seismic field of site 2	22
Summary and conclusions	24
References cited	27

FIGURES

1. Index map of the Powder River Basin, Wyo., showing location of Acme Mine 2
2. Map of the Acme Mine showing geophysical survey sites 1 and 2 3
3. Photographs of subsided Acme Mine 5
4. Graph showing representative net magnetism of various rock types 7
5. Graph showing first approximation of range of a maximized total-intensity magnetic anomaly as a function of distance from iron objects 8
6. Map of contoured magnetic field of site 1 9
7. Cross sections showing magnetic fields associated with buried junk and clinkers and subsided area at site 1 10
8. Graphs showing 16-inch normal resistivity logs, velocity distribution, and core densities from two boreholes 12
9. Map showing detailed topography of site 2 13
10. Cross section $C-C'$ through site 2 showing topographic surface and estimated position of mine openings with draw lines 14
11. Map of contoured magnetic field of site 2 15
12. Drawing showing magnetic anomalies calculated for mine-car rails in first and second entries and along cross section $C-C'$ of site 2, compared to measured magnetic field 16
13. Map showing electromagnetic field of site 2, in-phase component 17
14. Map showing electromagnetic field of site 2, out-of-phase component 17
15. Drawing showing the in-phase and out-of-phase electromagnetic components along cross section $C-C'$ of site 2 18
16. Drawing showing calculated effective depth of resolution for one-fourth skin depth of penetration for an electromagnetic source as a function of resistivity along cross section $C-C'$ 18

- 17-19. Map showing simple Bouguer gravity field of site 2, reduced at a density of:
 17. 1.70 g/cm³ 19
 18. 2.00 g/cm³ 19
 19. 2.67 g/cm³ 20
20. Drawing showing simple Bouguer gravity anomalies along *C-C'* for data reduced at three densities, compared with theoretical gravity anomalies computed for both air- and water-filled mine openings 21
21. Map of a soil arch in site 1 showing topography, location of seismic lines, and time-distance graphs 23
22. Location of seismic-refraction lines 1-5 along *D-D'* and *E-E'* at site 2 24
23. Time-distance curves and velocity-layering interpretation along seismic lines 1-3, of site 2 25
24. Time-distance curves and velocity-layering interpretation along seismic lines 4-5, of site 2 26
25. Time-distance graph and theoretical depth of penetration of a seismic wave 26

Geophysical Studies to Detect the Acme Underground Coal Mine, Wyoming

By C.H. Miller

Abstract

Adequate location maps are not available for some of the older underground coal mines in the Powder River Basin, Wyoming, nor for mines in other parts of the United States. These mines may subside and cause damage at the ground surface, or they may spontaneously ignite and consume coal deposits, polluting air and water. Consequently, techniques are needed for locating those potentially hazardous coal mines for which adequate maps do not exist.

The Acme underground coal mine is just north of Sheridan, Wyoming. Mining was begun in 1911 and abandoned in 1940. Coal was extracted from the relatively flat lying lower Monarch bed, which is about 6 m thick with no more than 12–20 m of overburden. The mine has burned and subsided over much of site 1, but site 2 was not subsided.

A ground-run magnetic survey of site 1 defined some prehistoric clinker (rocks heated by burning coal and made both brittle and very magnetic) that extended a few tens of meters into an outcrop, as well as some buried junk. The magnetic survey also delineated subsided ground, perhaps because of the mass effect of the broken terrain about the magnetometer or, perhaps, from magnetization of rocks by heat from burning coal escaping up subsidence fractures.

At the nonsubsided site 2, the data from magnetic, electromagnetic, gravity, and precise topographic surveys were reduced to individual contoured planimetric maps. None of the contour maps indicate the outlines of underground openings.

Theoretical magnetic calculations showed that although small iron objects such as tools could not be detected, large iron objects such as mine cars or heavy mine-car rails would produce much larger anomalies than were seen on the magnetic contour map. Calculations for the magnetic attraction of light mine-car rails at site 2, however, corresponded rather closely to one part of the measured magnetic field.

A long straight metal conductor buried less than 0.25 skin depths will significantly disturb an electromagnetic field. A range of skin depths was calculated for site 2 that essentially brackets the mine, but no significant equivalent electromagnetic anomalies were measured in the survey. Strong imaginary anomalies were measured over site 2, however, and these may possibly be attributed to ground-water variations between ground over the mine and ground away from it.

Theoretical gravity anomalies were computed for both air- and water-filled mine workings at site 2 assuming a rock density

of 2.3 grams per cubic centimeter. The calculations for the water-filled mine produced anomalies of about 0.4 and 0.9 milligal, considerably more than the possible error of 0.015 milligal, but neither calculation corresponded to a measured gravity anomaly.

Five seismic-refraction lines were run over site 2, and two velocity layers were determined: $V_{p2'}$ which represents the velocity of bedrock, and $V_{p1'}$ which represents the velocity of the overlying soil. The V_{p2} graph segments have a marked tendency to be nonlinear over the mined area and more linear away from the mined area. Both the depth to bedrock calculated from the seismic data and that calculated from velocity gradients measured in similar lithologies indicate, however, that the measured refracted seismic waves do not penetrate into the bedrock as deep as the mine level. Therefore, the nonlinearity of the V_{p2} segments may be caused by deformation above the mine, although deformation is not visible at the ground surface.

These studies are valuable as an aid in further research. Although none of the above methods adequately located the mine, some of them hinted at detection. In fact, it was shown that magnetic surveys can detect both the depth to which clinkers extend into an outcrop and iron in sufficient quantity. Although the surveys with interpretation were done systematically and with great care, they were largely unsuccessful, and hence they need not be duplicated. Variations of these methods as well as the application of different techniques may be fruitful, however.

INTRODUCTION

Exploitation of vast coal and other resources in the Powder River Basin, Wyo. and Mont. (fig. 1), has caused a rapid increase in population and in commercial and residential development in the basin since the mid-1970's. Studies therefore were implemented by the U.S. Geological Survey to aid in intelligent land use during this sudden expansion, which is expected to continue.

Abandoned underground coal mines in the Powder River Basin, as well as in other parts of the United States, present problems to land use. The land surface above these abandoned mines may eventually subside, thereby causing extensive depressions (Association of Engineering

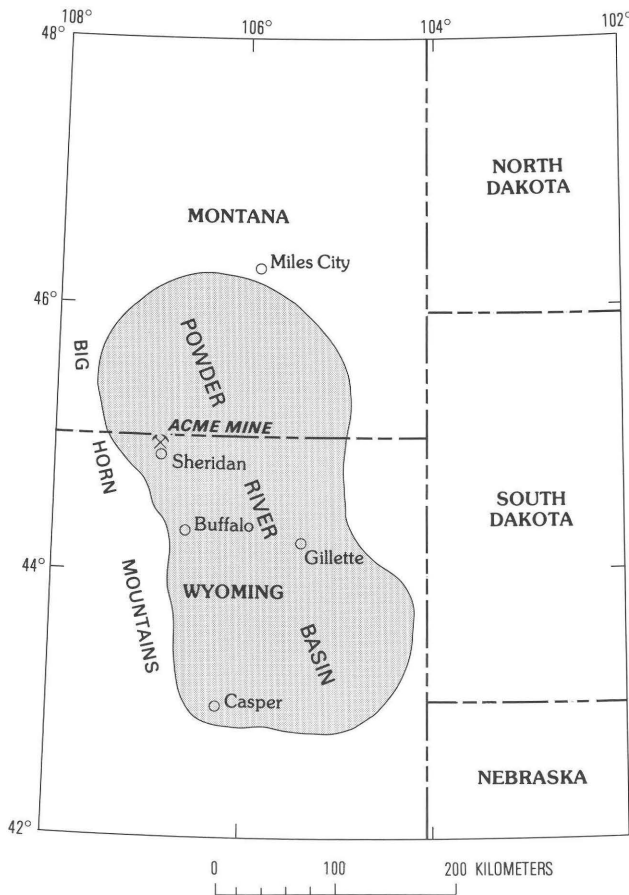


Figure 1. Powder River Basin, Wyo., showing location of Acme Mine.

Geologists, 1978; Dunrud and Osterwald, 1980). The resulting tension fractures around the depressions may also conduct air and water into the old mines and promote spontaneous combustion in the remaining coal. Underground fires pollute air and water, cause further subsidence, and may also burn into valuable unmined coal reserves.

Maps showing the location of abandoned underground coal mines are not always available, and thus the locations of some mines are unknown until they are detected by surface subsidence. Land that is underlain by coal mines but has not yet subsided may therefore erroneously seem suitable for construction sites.

The present report includes the results of geophysical surveys run during 1976 and 1977 over an underground coal mine in an attempt to provide geophysical techniques that may be used to locate these "lost" underground openings.

Two sites (fig. 2) over the old, underground Acme Mine were chosen for the geophysical surveys. A ground magnetic survey and a short seismic-refraction line were run at site 1. Gravity, electromagnetic, seismic-refraction, and leveling surveys as well as a magnetic survey were run at site 2. In early 1978, the coal in the mine near site

2 was burning so rapidly that a previously constructed firebreak strip mine was continued south and southwest of the site in order to save the unmined coal south of the break. This mining activity forced the cessation of further geophysical surveys at site 2.

The findings from these present studies may have application to other searches for buried cavities by geophysical methods. Manmade cavities created by underground gasification of coal or by underground solution of salt deposits, for example, cannot accurately be located in many instances. The detection by earlier geophysical methods of naturally occurring underground cavities, including sinkholes and caverns in carbonate rocks and tubes in lava, has also met with only limited success (U.S. Army, 1977, 1981).

ACKNOWLEDGMENTS

Access to the survey sites was permitted by personnel of Peter Kiewit Sons' Co. and Big Horn Co., Sheridan, Wyo., and the Padlock Ranch, Dayton, Wyo.

T.F. Bullard, S. Kanizay, W.M. Miller, J.K. Odum, F.W. Osterwald, and A.L. Ramirez participated in the geophysical field surveys and data reduction. All these participants except W.M. Miller were employees of the U.S. Geological Survey at the time of the surveys and data reduction.

Most of the survey instruments were borrowed: magnetometer, E.R. Landis, U.S. Geological Survey; gravimeter, D.L. Healey, U.S. Geological Survey; seismograph, U.S. Bureau of Land Management; and electromagnetometer, G.V. Keller, Colorado School of Mines.

Technical advice was provided by the following USGS personnel: H.D. Ackermann, seismic refraction; G.D. Bath, magnetics; R.R. Wahl, gravity; and R.D. Watts, electromagnetics. F.W. Osterwald, U.S. Geological Survey, provided information on principal facts and geology of the Acme Mine, and reviewed the manuscript both with the other advisors and after their critiques had been received and incorporated.

The author thanks all of these people and organizations for their support. The accuracy of the final product, however, is the sole responsibility of the author.

THE ACME MINE

The Acme Mine is just north of the former town of Acme (figs. 1, 2), which is about 13 km north of Sheridan, Wyo., in the northwest part of the Powder River Basin.

The major coal deposits in the area of the mine are in the Tongue River Member of the Fort Union

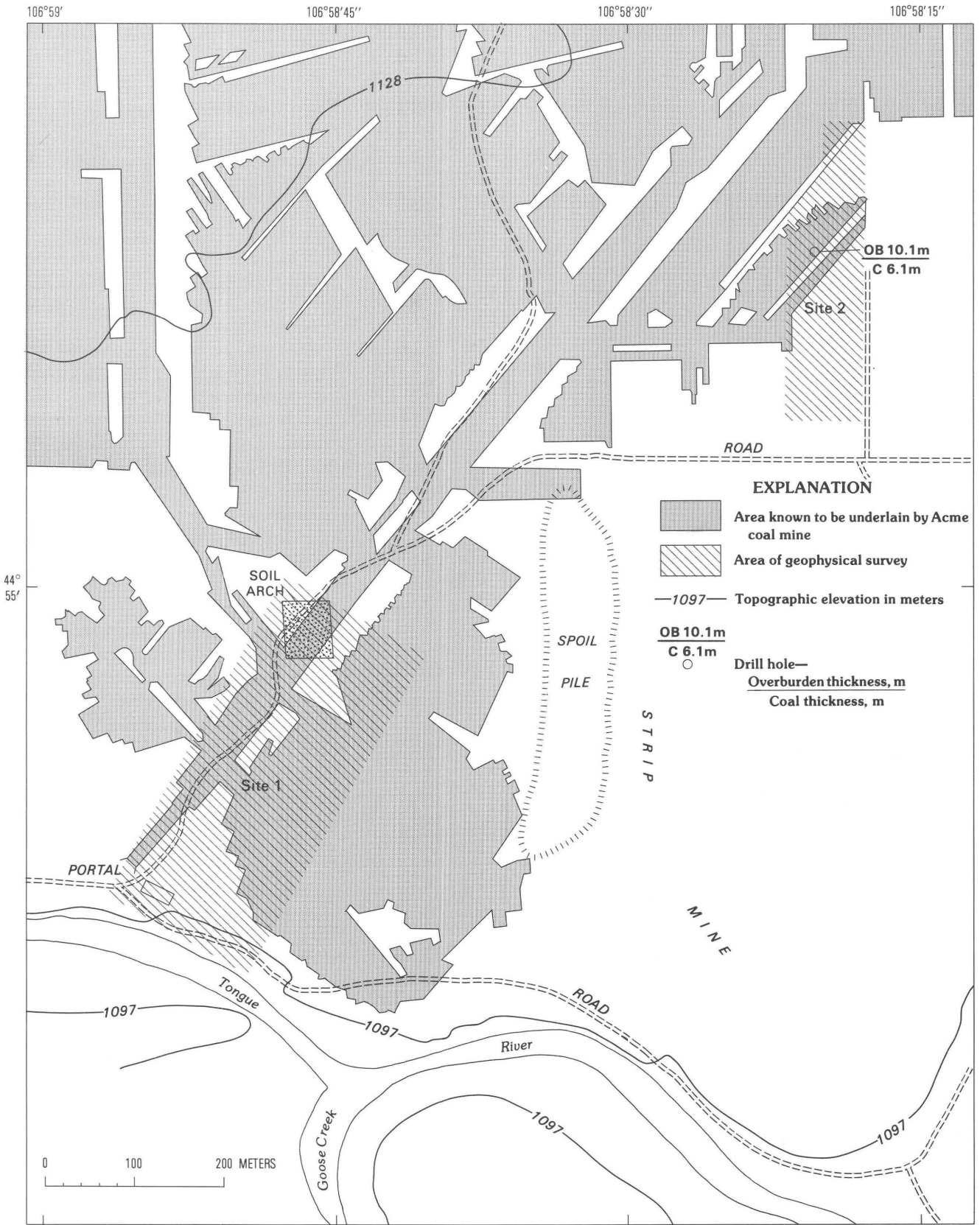


Figure 2. Acme Mine, showing geophysical survey sites 1 and 2.

Formation of Paleocene age (Mapel, 1959; Dunrud and Osterwald, 1980). The rocks of the Tongue River Member consist of soft mudstones, siltstones, and friable sandstones, as well as the coal beds. The coal beds vary in thickness from less than 1 m to as much as 17 m.

Many coal beds in the Acme area, as well as in other parts of the Powder River Basin, were burned along their outcrops during prehistoric time, and the resulting intense heat has baked and fused the overlying sedimentary rocks into clinkers (Rogers, 1917; Bauer, 1972). In this report, clinker deposits are meant to include all baked and fused sedimentary rocks as well as any coke and ash residue from the burned coal. Clinkers are brittle and very magnetic.

Surficial deposits at the survey sites include alluvium, colluvium, and regolith derived mainly from the relatively soft rocks of the Fort Union Formation. Thickness of the surficial deposits was observed in most scarps around subsidence pits to be less than 5 m.

The Acme Mine was begun in 1911 and abandoned in 1940. During its life span, the mine was extended over about 5.8 km². Coal was extracted from the lower Monarch bed, which is about 6 m thick with 10 m of overburden at site 2, according to a drill-hole and coal-mine map furnished by the Big Horn Coal Company (written commun., 1982). This coal bed dips less than about 1° to the east and northeast according to elevations on the floor shown on an older mine map (Sheridan-Wyoming Coal Company, 1938). These floor elevations are assumed to be parallel with the lower contact of the coal bed.

The coal was mined by the room-and-pillar method, and perhaps less than 50 percent of the coal shown in the plan view was extracted. The rooms tended to be about 3–4 m high and 2.5–4 m wide. About 1–1.5 m of coal were left in both the ceiling and floor, evidently to provide stability. C. R. Dunrud (oral commun., 1983) related conversations with some of the original mine personnel, who pointed out that manmade ground support was not installed in the working entries except for supporting electric lines, but it probably was used in the main entryways. Some of the roofs were evidently flat, although old photographs of the mine interior show some arching. The roofs were presumably arched both naturally by slight caving and intentionally, for strength and mining convenience.

Kuzara (1977, p. 111–126) related that the coal was mined by undercutting the working face of coal with “short-wall” machines before the coal was shot down and loaded in cars by hand. The cars were then dragged to the main entryways by horses and taken out of the mine by motor cars that were evidently electrically powered. The main tunnels were electrically lighted, and the mine had a complete system of telephones with a phone at every point from which coal was being taken. The main tunnels also had “tracks for the motors and cars with 65-lb

[per 1-yd length] rails throughout; the branch lines into the working chambers [were] temporary and lighter steel [was] used.”

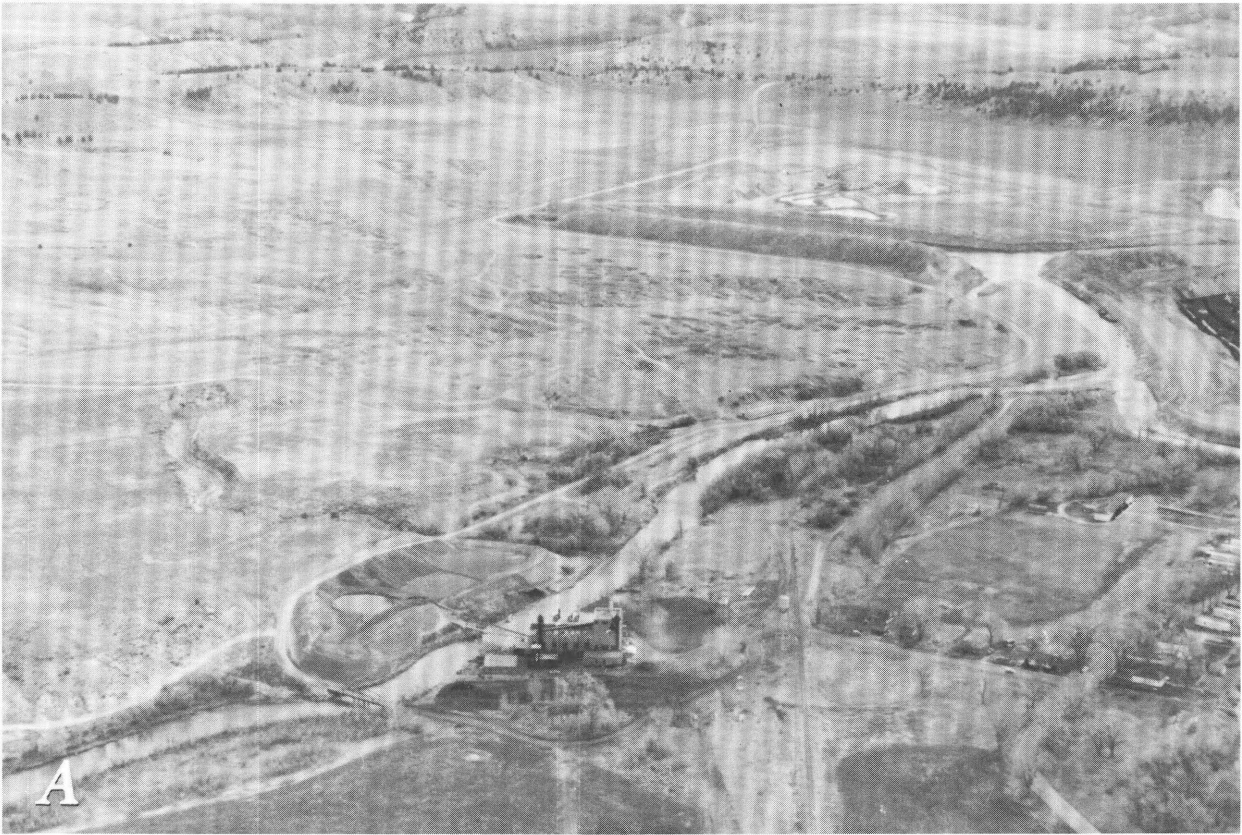
Much of the mine has subsided and left broad topographic depressions (figs. 3A and 3B) that may span many rooms and entries (Dunrud and Osterwald, 1980). Localized pits and troughs are also included within the broad depressions, as well as along tension cracks around the large subsidence depressions. The main subsidence mechanism is apparently broad collapse of the mine roof with consequent stoping over individual underground openings. An original underground opening may “migrate” upward as far as the topographic surface and become manifested as a pit or trough. The pits and troughs seem to develop most easily over the intersections of underground openings, where the raveled and collapsed debris has migrated laterally into rooms, drifts, or crosscuts. Conversely, relative stability may occur over pillars or main entries that were still well supported after the mine was abandoned. The road that bears northeast from the portal and through site 1 (fig. 2), for example, is over the main haulageway of the mine. The manmade support in this main entry was apparently not removed before the mine was abandoned, and therefore the ground surface over it is still relatively unaffected by subsidence.

Most of the topographic evidence of subsidence within the area of figure 2 is south of the 1128-m contour. Overburden above the mined coal bed in this area of subsidence is less than about 40 m, but the overburden north of the 1128-m contour shown in figure 2 may be as much as 70 m thick. Overburden thickness above the coal at the two geophysical survey sites (fig. 2) is estimated at 10–20 m, based on mine and topographic maps.

Subsidence is evident over nearly all of site 1 where mining has been done. Any underground openings that remain at mine level are presumably filled with air rather than water because no water can be seen at the adit and also because any water introduced into the mine would tend to drain down dip to the east.

Subsidence is not apparent at site 2 (fig. 2), except at the extreme northern tip of the area and outside site 2 on the west, even though much of the site was undermined. The reason for the lack of subsidence over the mines at site 2 is unknown. If the mining at site 2 was the same age as that under the subsided area and the

Figure 3 (facing page). Photographic views across subsided Acme Mine. *A*, An oblique view northeast across map of figure 2; site 1 is in center of photo between power plant and large spoil pile and site 2 is in upper part of photo and immediately beyond northern tip of spoil pile. Photograph by F. W. Osterwald, April 1976. *B*, Northeast view across part of mine that is about 2.5 km north of spoil pile of *A*; this part of mine was burning in 1980 both at depth and at ground surface with accompanying subsidence, explosions, and air pollution. Photograph by F. W. Osterwald and J. B. Bennetti, Jr., February 1980.



ground support was the same, then the ground at site 2 should have likewise subsided. This is not the case, however. The mining at site 2 must have been done after the mining under the northern tip and to the west because the nonsubsided portion of site 2 is peripheral to the other mining. Most of the Acme Mine is, indeed, constrained by boundary lines of partial sections and ownership, but the mining at site 2 was not completed over all of its section. An older mined area would be more prone to failure than a significantly newer mined area.

Another possible explanation for the lack of subsidence of site 2 is that the pillars may not have been mined as the miners "backed out" and abandoned that area. Yet another possibility is a change in geology. Relatively competent bedrock over site 2 may have contributed to its support and therefore retarded subsidence.

The amount of water that occupied the original underground openings under site 2 at the time of the surveys is unknown. Any water introduced into the relatively nonsubsided area at site 2 might be trapped there because there is no outlet downdip to the east and northeast (fig. 2). Any water introduced into the subsided area, however, would probably be diverted downdip and into openings that are continuous to the east and northeast and out of the area.

At the time of the geophysical surveys in 1976 and 1977, a local inhabitant reported that snow readily melted over most of site 1 and that visible steam issued from some of the subsidence-caused fractures. Therefore either some of the unmined coal under site 1 was apparently burning, or warm air was conducted through the underground openings and to the ground surface by subsidence fractures. Site 2 showed these same heat characteristics at the subsided part at the northern tip of the site but not at the nonsubsided southern portion.

GEOPHYSICAL SURVEYS

Sites 1 and 2 (fig. 2) were both nearly free of man-made disturbances and objects such as powerlines, fences, and vehicular traffic that might interfere with geophysical surveys.

Site 1 was selected for a magnetic survey because of the possible presence of abandoned iron objects in the mine. Also, most of the area was collapsed and much of the unmined coal was burning, with the possibility that the rocks along subsidence fractures would be magnetized by escaping heat. The undulating terrain of the subsided area would invalidate gravity, seismic, and electromagnetic surveys, which are sensitive to topographic relief.

Site 2 was selected for detailed study because subsidence was visible only at the northern tip of the site. Topographic relief at site 2 is relatively low, so the effect of either naturally rough terrain or subsided ground on

the geophysical survey data would be minimized. The site was desirable also because the surveys would straddle the boundary of the known mined area.

Both magnetic and electromagnetic surveys were run at site 2 because iron objects may have been abandoned in the mine and also because the magnetic and electromagnetic fields over the nonsubsided area may have been changed either by the underground openings or by burning coal. Gravity and seismic surveys were run to detect the underground openings; a leveling survey was run in conjunction with the gravity survey for use in the data reduction and to define any subtle subsidence trends that were not visible.

Geophysical techniques and principles are discussed in this report in the following order: magnetics is discussed in relation to site 1, although a magnetic survey was also run at site 2; electromagnetics, gravimetry, and seismology are discussed in relation to site 2 because these surveys are essentially unique to that site, except for a relatively small seismic survey at site 1 (fig. 2).

Site 1

Magnetic Anomalies Caused by Heating Rocks and by Iron

Location surveys of abandoned coal mines have been run with magnetometers to locate rocks that have become magnetic when heated. D.E. Watson and D.B. Hoover (written commun., 1977) have surveyed burning coal mines, including part of the northern part of the Acme Mine, in an attempt to locate these burn fronts.

When gray clastic rocks are heated, they tend to turn some shade of red or dark brown and become more magnetic. According to D.E. Watson (written commun., 1976) the red hue mostly can be attributed to iron-oxide silicates, but the minerals that mainly contribute to the thermal-remanent magnetism are mostly ilmenohematites and titanomagnetites. The magnetic domains of these minerals are originally in a relatively random orientation, but heating reorients the domains so that they are parallel with the Earth's field at the time of heating and the net magnetization is greatly enhanced, along with other possible changes. The temperature does not have to exceed the Curie point in order for the rocks to be remagnetized.

The distribution of magnetization in various rock types is compared in figure 4. The net magnetization of clastic rock is dramatically increased by several orders of magnitude when the rock is heated and the magnetization appears to be related to the degree of baking and fusing. The resulting clinkers are among the most magnetic rocks found in nature. The degree of magnetization caused by heating along subsidence fractures within clastic rocks, however, is unknown.

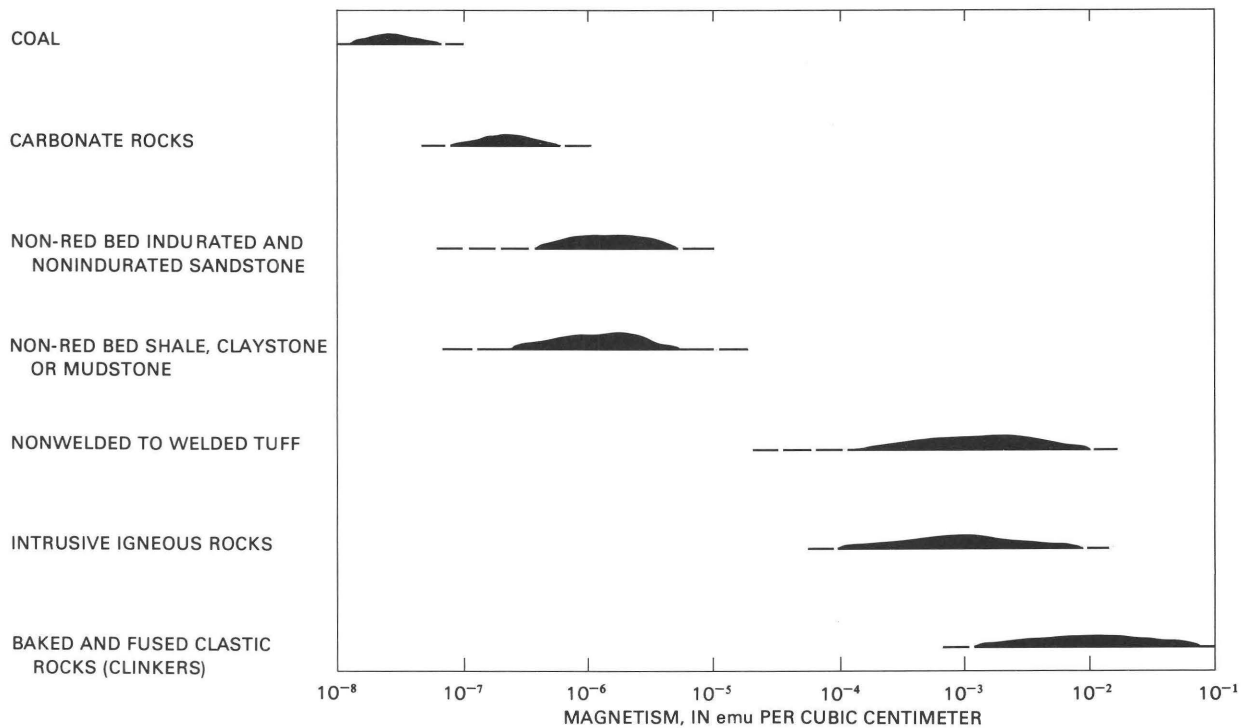


Figure 4. Representative net magnetism of various rock types (D.E. Watson, written commun., November 1976).

Iron objects abandoned in mines also cause magnetic anomalies that may be detected at the ground surface. Figure 5 is a first approximation of the range of a maximized total-intensity magnetic anomaly as a function of distance from iron objects.

Figure 5 indicates maximum anomalies for dipole objects that range in size from small tools to a mine car and for objects with lines of dipoles, such as mine-car rails. The magnetic attraction of dipole objects decreases as the inverse *cube* of the distance to the magnetometer. The first approximation formula (Briener, 1973) for this dipole case (objects of finite dimensions such as tools or a mine car) is

$$T = \frac{kFV}{r^3} \quad (1)$$

The magnetic attraction of an object represented by a long line of dipoles decreases as the inverse *square* of the distance. The first approximation formula for a line of dipoles (objects of one infinitely long dimension such as a mine-car rail) is

$$T = \frac{kFA}{r^2} \quad (2)$$

where F is the Earth's field, about 57,770 gammas at the time site 2 was surveyed; T is the total magnetic intensity anomaly in gammas; k is magnetic susceptibility, about

25 for "hard" steel, in cgs (centimeter gram second) units; V and A are volume and area, respectively, in cgs units; and r is the distance between the magnetometer and the iron object, in centimeters.

Henshaw (1977) and Gallagher and others (1978) ran magnetic surveys as well as other geophysical surveys over abandoned vertical mine shafts. The shafts had been backfilled with iron objects as well as with soil of different magnetic properties than the surrounding rock, but no surface trace was found at the shafts. These surveys yielded positive results where the shaft fillings contained a significant amount of iron objects. The only known entry to the Acme Mine in the site areas is horizontal rather than vertical, but the subsidence pit over it has been backfilled with iron objects and soil.

Magnetic Survey and Magnetic Field Characteristics

A total magnetic intensity survey was run over the grid of site 1 (fig. 6) with a portable proton magnetometer. Readings were taken at about 10- or 30-m intervals with the sensor at a constant height of about 2.1 m above ground. Individual readings of total magnetic intensity were read to an accuracy of about ± 1 gamma (± 1 nT (nanotesla)). The readings were reduced to a base station value of 58,634 gammas. Base readings were repeated within 20 minutes of the initial reading at an accuracy of ± 4 gammas, and this base drift was linearly distributed over the station readings. The results are

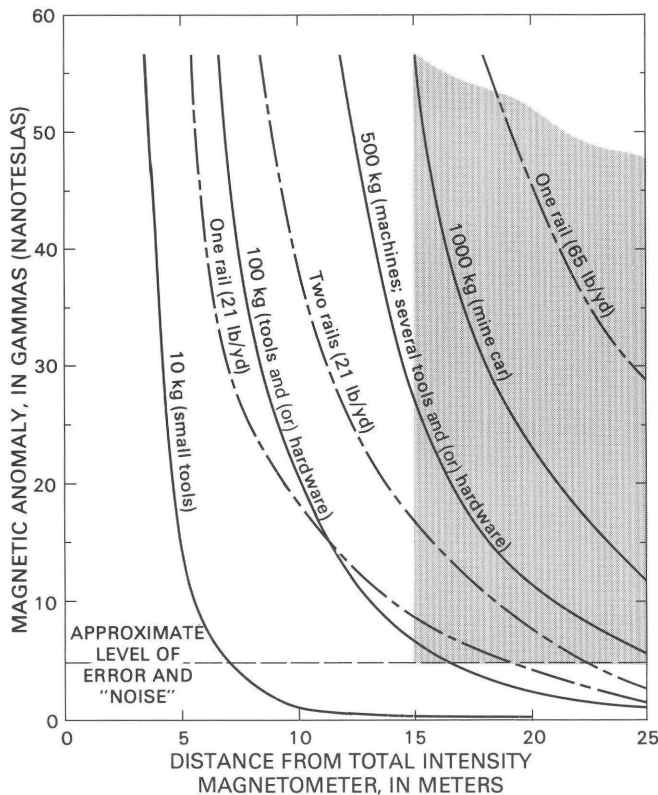


Figure 5. First approximation of range of a maximized total-intensity magnetic anomaly as a function of distance from iron objects. Objects are assumed to be on floor of the Acme Mine, 15–25 m (shaded area) below magnetometer at ground surface. Mine rail weights are in conventional units.

shown in figure 6, a map of the contoured magnetic field, and figures 7A and 7B, cross sections showing anomalies, ground surface, buried materials, and mine workings.

The magnetic field of site 1 shown in figures 6 and 7B is divided into three broad anomalies:

1. The anomaly characterized by the 200-gamma contour interval, which is associated with the area of outcropping clinkers at the south end of the site (fig. 7B). This anomaly also includes a more localized anomaly caused by a junk pile (fig. 7A) in the southwest corner of the site.
2. The anomaly characterized by the 50-gamma contour interval associated with the relatively major subsidence area in the central part of the site.
3. The anomaly characterized by the 5-gamma contour interval associated with the relatively minor subsidence area at the north end of the site.

Some localized magnetic anomalies are also evident around near-surface objects that are made of iron. The known objects made of iron include the steel drill-hole casings in the west-central part (fig. 6) and the junk in the southwest part of site 1. No rails, steel supports, or other objects made of iron could be seen within 6 m inside the main portal.

The clinkers at the south end of site 1 are exposed at a scarp along the north side of the Tongue River (fig. 2). The scarp is as much as 15 m high within site 1. Clinkers may crop out anywhere in the exposed section, although they are more evident in the upper part of the scarp.

The magnetic anomaly (figs. 6 and 7B (B–B')) that is produced by these clinkers is characterized by the 200-gamma contour interval. It has a magnitude of at least 600 gammas and is as much as 60 m wide. The width at the midpoints on the flanks of the anomaly, however, may more accurately measure the width of the mass of clinkers (Hasbrouck and Hadsell, 1976); this width is about 40 m. The anomaly does not extend over the subsided area, which implies that the clinkers extend only about 40 m into the outcrop and that the coal could only be mined as far south as the clinker contact. Subsidence, therefore, apparently begins approximately at the contact of the coal with the clinkers.

Figure 7A (A–A') shows the magnetic anomaly associated with the buried junk pile in the southwest part of site 1 (fig. 6). The junk that is partly composed of iron includes one or two car bodies, some stoves and refrigerators, and various smaller objects such as cans, all of which were dumped in the subsidence pit over the entryway of the mine. The maximum amplitude of the anomaly over the junk pile is at least 4,800 gammas, and its width is about 3–4 m at the midpoints on its flank.

The junk was visible during the original magnetic survey of site 1. It was buried later by no more than about 4 m of soil, and then the magnetic profile was run. The magnetic profile along A–A' of figure 7A demonstrates the ease with which junk buried in these pits as well as other pits can be identified. The profile may also give some indication of the amount and proximity of iron objects in pits.

Any iron used in mining but abandoned in an underground mine, however, is expected to be present in much smaller quantities and in less concentration than in the junk pile along A–A' (fig. 7A), and it would almost certainly be buried deeper unless it were in shafts. The resultant anomalies caused by iron abandoned in mines are discussed more fully in conjunction with site 2.

The anomaly with a contour interval of 50 gammas in the central part of site 1 is of only slightly greater value (about 350 gammas) than the maximum residual of the 5-gamma-contour anomaly (about 110 gammas) at the north, although the latter anomaly may appear to be more complex because of its smaller contour interval (fig. 6). Neither of the broad central or northern anomalies appears to be controlled by mine drifts or rooms because the associated anomalies seem to be randomly oriented. The boundary between the central and northern anomalies, however, coincides with the general boundary between the areas of major and minor

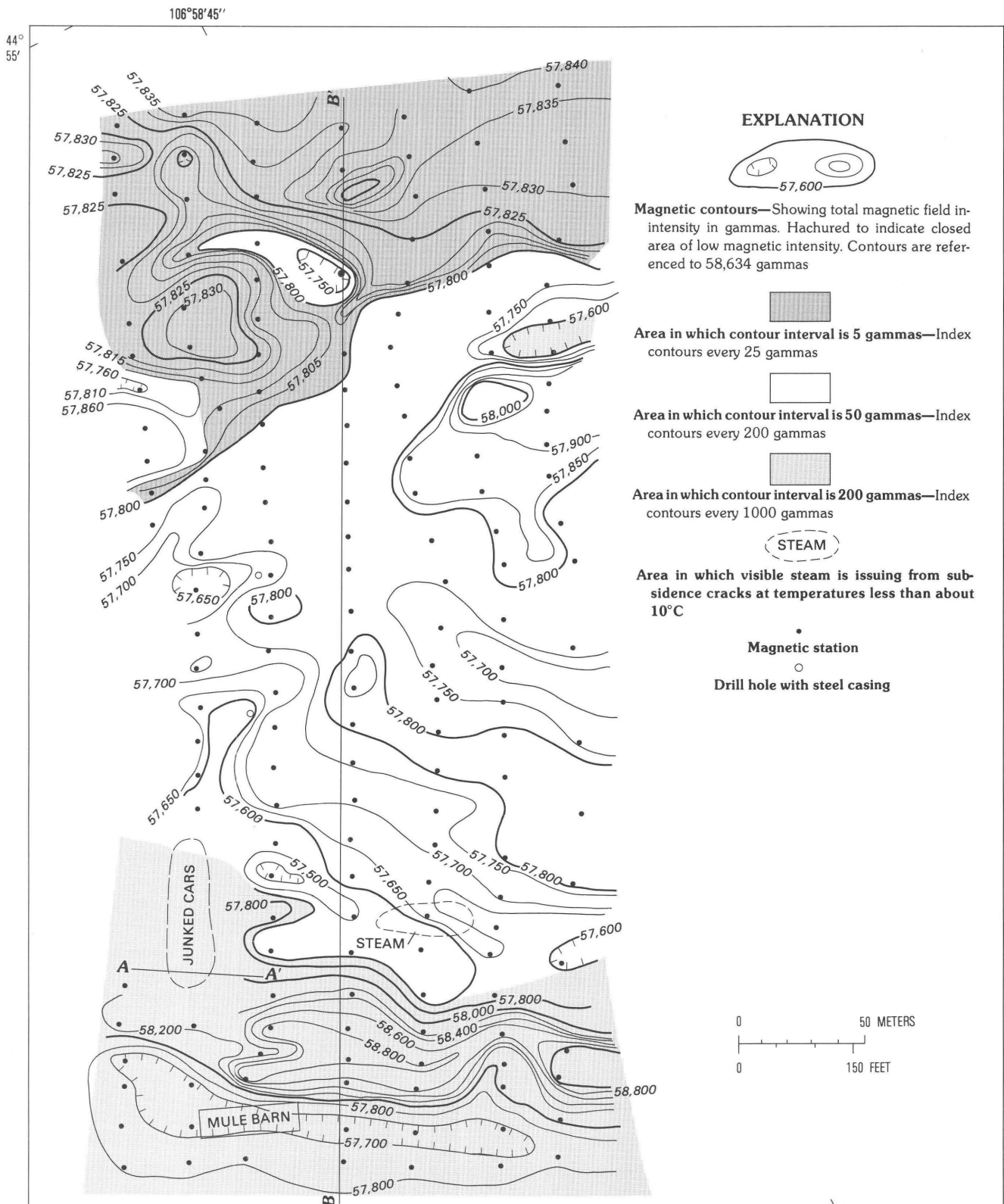


Figure 6. Map of contoured magnetic field of site 1. (See fig. 2 for location of site 1.) Section A-A', B-B', figure 7.

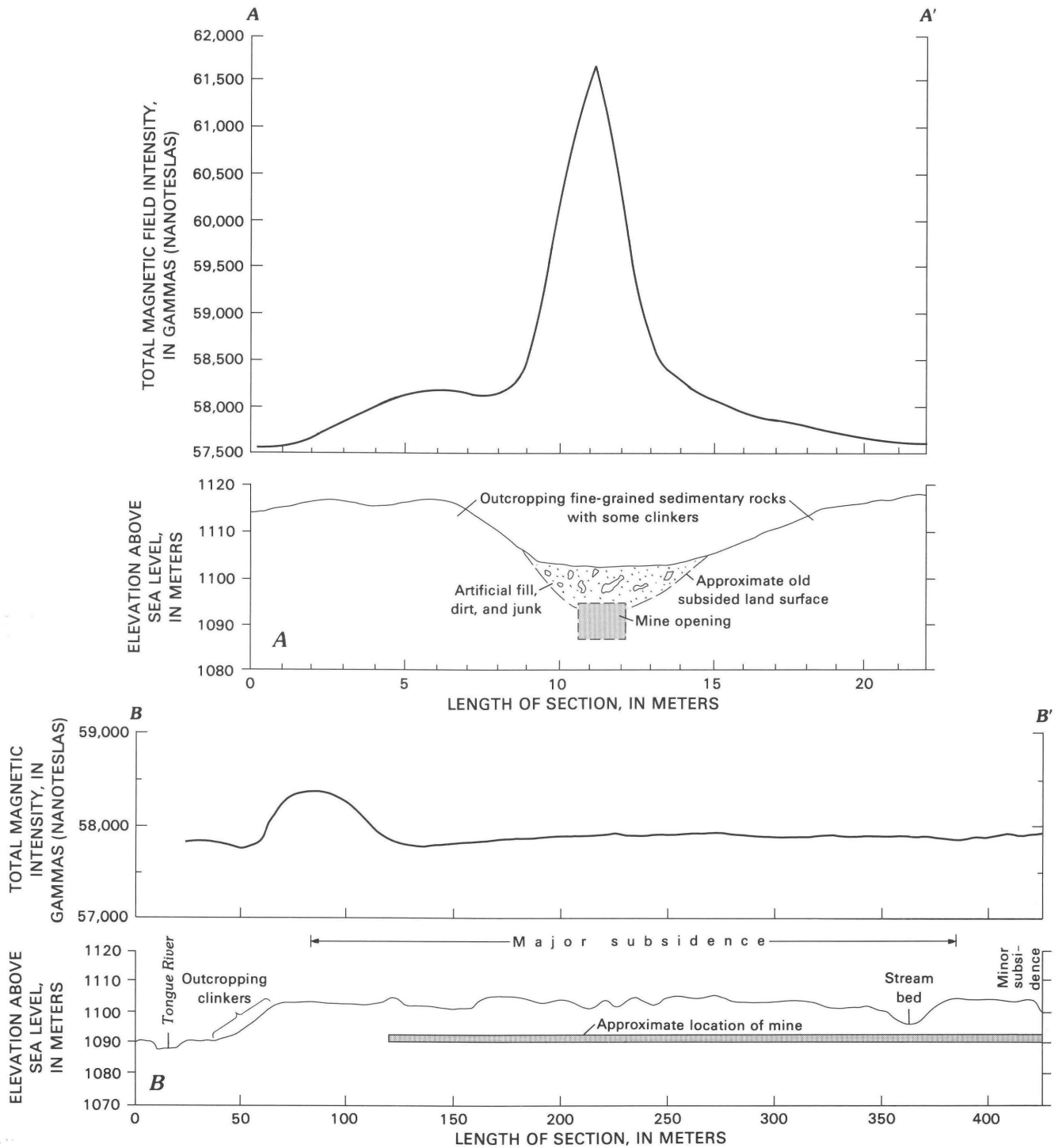


Figure 7. Magnetic fields associated with A, buried junk (A-A') and B, clinkers and subsided area (B-B') at site 1.

subsidence (figs. 6, 7B). The slightly higher amplitude of the 50-gamma-contour anomaly in the central part of site 1, therefore, appears to be related to the area of major subsidence. The cause of this greater anomaly over the subsided area is unknown. Perhaps any heat in the mine

below the area of greater subsidence could more easily escape up subsidence fractures and magnetize nearby rocks, or perhaps a terrain effect caused by the undulating topography of the subsidence pits influenced the magnetic measurements.

Site 2

The Acme Mine surveys at site 2 include measurements of topography, magnetics, electromagnetics, gravity, and seismic velocity. Some of these measurements essentially can be assessed independently; others need supporting information. Separate measurements or at least reasonable estimates of resistivity for the electromagnetic surveys are needed, and a vertical profile of velocities is desirable for the seismic surveys. These supporting data are commonly collected from nearby boreholes, but unfortunately no borehole information of this type was available near the Acme Mine.

Geophysical data were available, however, from two boreholes away from the Acme Mine but drilled in similar rocks. The data from these holes are reproduced in figures 8A (borehole B-1 (Farrow, 1976)) and 8B (borehole S-2 (Farrow, 1980)). Borehole B-1 penetrated the Wasatch Formation and borehole S-2 penetrated the same geologic formation (Fort Union) as was mined at site 2. The lithology of the Wasatch and Fort Union Formations is very similar. Borehole S-2 is 13 km south of the mine at Sheridan, Wyo., and B-1 is 67 km south. Because the lithologies at the boreholes and at the undisturbed ground at the mine are similar, the geophysical data seem to be at least indicative of some properties at site 2.

Figure 2 shows the general outline of the Acme Mine in 1938 (Sheridan-Wyoming Coal Company, 1938) and the generalized topography of site 2. Figure 9 shows the detailed plan of the mine at site 2 as well as the detailed topography, and figure 10 shows a cross section through figure 9. The horizontal accuracy of the mine map is apparently within 10 m. The mine map presumably was updated to include all mining at site 2. The mine rooms are estimated to be about 3–4 m high, and their average depth of burial at the southern boundary along the cross section of figure 10 is estimated to be about 11 m.

The ground-surface area affected by subsidence is commonly greater than the mined area where all the coal has been removed. The draw angle (fig. 10) is measured from the vertical and includes all the subsidence-caused deformation at the ground surface down to the outer boundary of the mine opening that caused the subsidence. The angle of break is also measured from the vertical. The break line connects points of maximum tensile stress and strain from the ground surface down to the edge of the mine workings. The draw angle may range from 0° to 35° in many coal mines in the West, depending on overburden thickness, mining methods, geology, and topography. However, the draw angle for abandoned mines around Acme, where the overburden is less than about 60 m, is steep to near vertical (Dunrud and Osterwald, 1980).

Topographic Survey

The topography of site 2 (figs. 9, 10) was precisely surveyed in order to accurately reduce gravity data and to define any subtle patterns in the topography caused by subsidence over the mined area. The grid of site 2 was laid out with a transit and tape, and its horizontal accuracy is about ± 0.3 m. The elevations of the grid were leveled to an accuracy of about ± 0.015 m.

According to A.A. Matilla (U.S. Geological Survey, oral commun., 1976), aerial photographs were taken of the Acme Mine in the early to middle 1940's. He recalled that in 1949 he could clearly see the outline of drifts, pillars, and rooms on the photographs over some parts of the Acme Mine; but when he drove over the mine in the same year, he could see no surface trace of subsidence on the ground. The detailed topography of figures 9 and 10 shows a relatively featureless slope to the southeast. There is no particular pattern to the contours, however, that suggests that they are controlled either by subsidence or by small and local intermittent streambeds.

Magnetic Survey and Magnetic Field Characteristics

A magnetic survey was run over the grid of site 2 using the same portable magnetometer and the same field techniques that were used at site 1. The readings at site 2 were also corrected for drift and referenced to the same base-station value of 58,634 gammas as the readings at site 1.

The contoured magnetic field of site 2 is shown in figure 11, and a cross section ($C-C'$) through the site is shown in figure 12. There is no prominent isogamma contour pattern that suggests subsurface control of the magnetic field.

A relatively prominent residual magnetic low (57,620 gammas) of less than about 15 gammas exists over the "working rooms" (in the center of the area of fig. 11) of the nonsubsided area. A very general high (57,620 gammas) of about 10 gammas is positioned over the main and bypass entries in the older workings (subsided) to the northwest of the low, and another high (57,620) of perhaps 15 gammas is over the first and second entries in the newer workings (nonsubsided) to the southeast of the low. These two general magnetic highs may be caused by abandoned iron objects in the first and second entries and (or) changes in the amount of magnetite in the intervening sedimentary rocks of the overburden. In addition, the anomalous high over the subsided older workings may be influenced by magnetization caused by heat from mine fires escaping up subsidence fractures.

The graph of the first approximation of magnetic intensity (fig. 5) indicates that at least two 21-lb/yd rails must be present in the mine at site 2 in order to be reliably

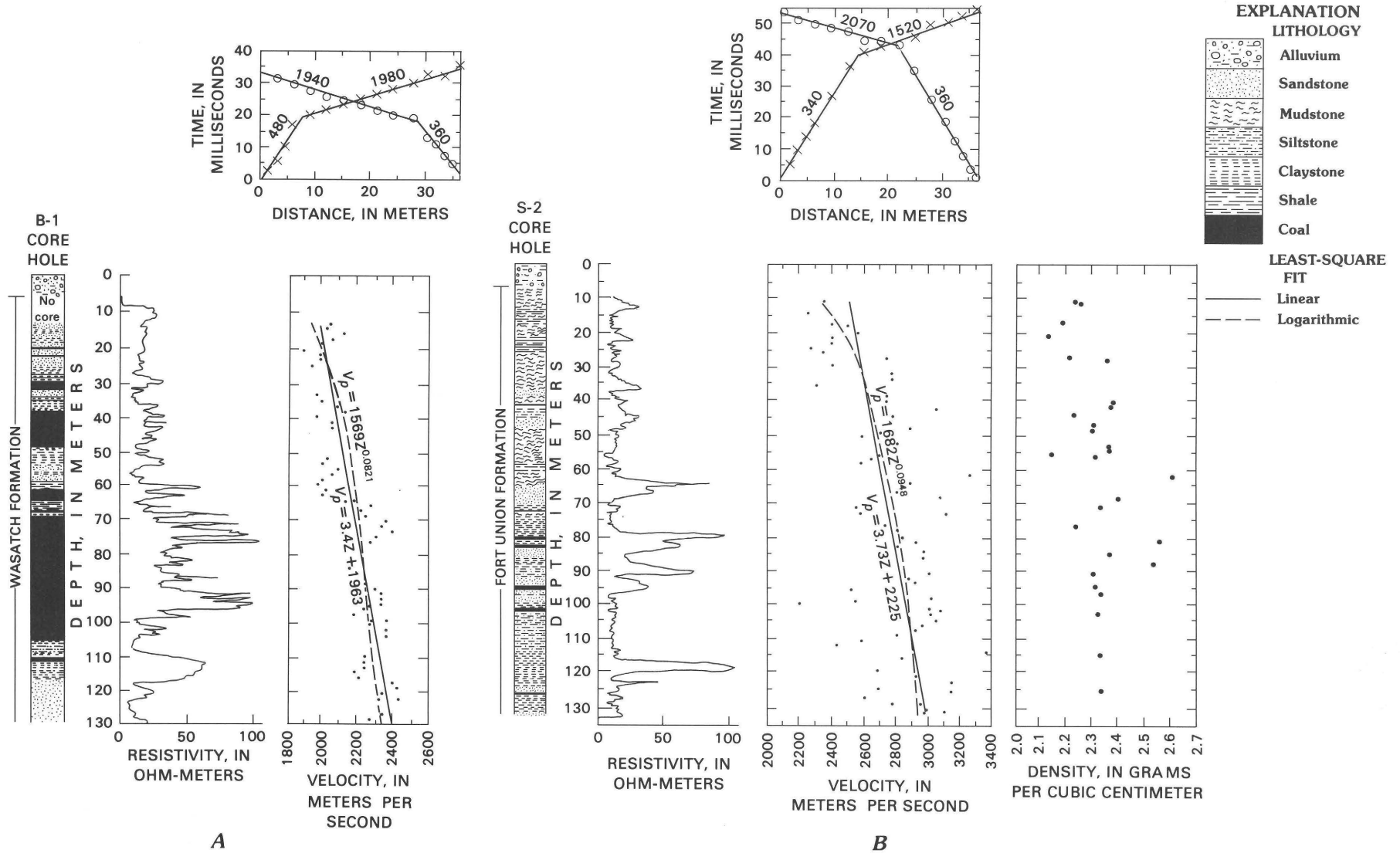


Figure 8. Sixteen-inch normal resistivity logs, velocity distribution (least-squared data from boreholes and data from surface-run seismic surveys at the boreholes), and core densities from two boreholes: A, B-1 at Buffalo, Wyo., and B, S-2 at Sheridan, Wyo. Although both boreholes are some distance from Acme Mine, S-2 borehole is in same unit as mine (Fort Union Formation), and B-1 borehole is in a lithologically very similar formation (Wasatch Formation). On least-squared fit, V_p , compressional wave velocity in meters per second; z , depth in meters. On surface-run seismic surveys, numerals on curves, compressional-wave velocities in meters per second; x , \circ , arrival times. These basic data are used in reduction and interpretation of electromagnetic surveys.

detected; however, it also indicates that just one 65-lb/yd rail or one 1,000-kg mine car would create relatively very large anomalies. Because the magnetic anomaly map of figure 11 does not depict such large anomalies, two 21-lb/yd rails in both the first and second entries of site 2 have been assumed to be a more reasonable situation for modeling purposes.

Magnetic anomalies were calculated for mine-car rails in both the first and second entries of cross section C-C' in figure 12. The calculations assume that there is only one set of continuously joined rails per drift and that each set can be represented by one solid, horizontal steel cylinder. A horizontal cylinder magnetized by a steeply dipping (about 75°) Earth's field would behave as a monopole, although the rails are a continuous line of dipoles. Equation (2) was used to approximate rails along cross section C-C' by substituting the same magnetic and cylinder values used to compute the graph of figure 5.

The magnetic anomalies for the main and bypass drifts were each computed separately as well as together, and the results are plotted over the respective drifts and compared to the measured total-Earth's field in figure 12. The configuration and amplitude of the computed anomalies generally match those of the measured magnetic field. Furthermore, the peaks are positioned so that they could be caused by iron-made objects in the two drifts. There is enough ambiguity in the magnetic prospecting method, however, that other evidence should be collected and interpreted before the presence of iron objects in the main and bypass drifts can be concluded.

Electromagnetic Survey and Electromagnetic Field Characteristics

An electromagnetic survey was run over the grid at site 2 using a Slingram apparatus (Keller and Frischknecht, 1970). This method uses two portable coils that are held horizontally and in the same plane. One coil is a transmitter and the other is a receiver; they are connected by an electric wire. When the coil of the transmitter is energized, its primary electromagnetic field induces eddy currents into the ground. The resulting eddy currents produce a secondary electromagnetic field. The primary field is compensated for by referencing along the electric wire, and the resultant secondary field is detected and resolved into two components with 90° separation: (1) the in-phase or real component and (2) the out-of-phase or "imaginary" component. The components are expressed arbitrarily in percentage of secondary field strength; the real component is referenced to 100 and the imaginary component is referenced to 0. The ratio of the in-phase anomaly to the out-of-phase anomaly, as measured in homogeneous earth, is small for poorly conductive earth and large for conductive earth; however, this ratio also depends on the geometry and conductivity

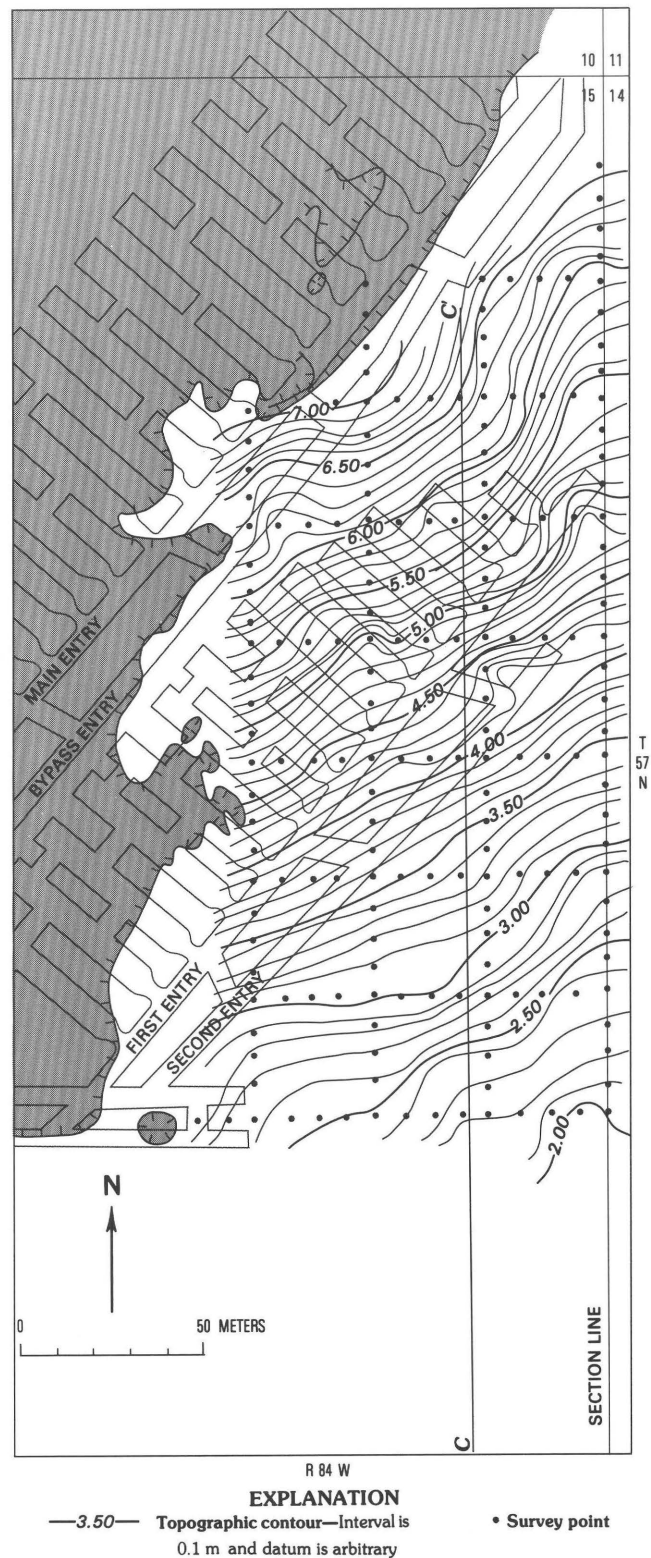


Figure 9. Detailed topography of site 2, Acme Mine, showing passages (mine map, Sheridan, Wyoming Coal Company, 1938), limits (hachured line) of visible broad surface subsidence (shaded) and detailed topographic survey at site 2, which is away from the visibly subsided area. Limits of theoretical deformation (draw line) above mine passages are nearly vertical for these rocks but detailed topography does not indicate actual subsidence. Section C-C', figure 10.

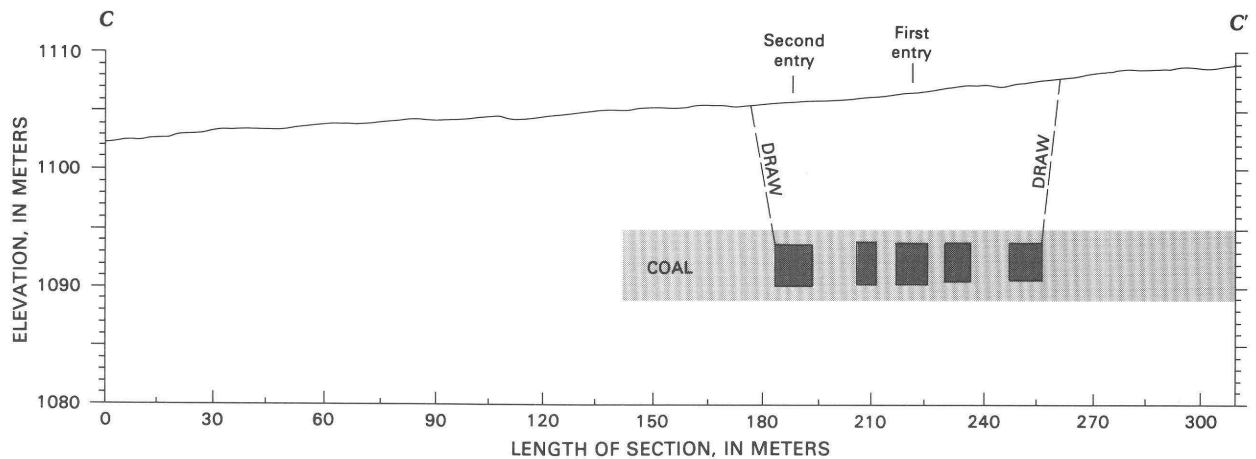


Figure 10. Cross section C-C' (fig. 9) through site 2 (fig. 9) showing topographic surface and estimated position of mine openings with draw lines (theoretical limits of subsidence). Subsidence was not indicated by detailed measurements of topographic surface.

of layers as well as the frequency of the primary electromagnetic field (Parasnis, 1966).

The apparatus had ostensibly been calibrated over "neutral ground" prior to being loaned to the investigators, but an approximate check was still made at site 2. This check was done over smooth terrain but away from possible effects of mine subsidence. Essentially no adjustments were needed as indicated by the check. Readings taken during the mine survey were taken at input frequencies of both 440 and 1,760 Hz; the readings taken at the low frequencies exhibited instrument noise, so the higher frequency data were used in the analyses.

The survey was advanced in a series of straight lines that were mutually parallel with north headings and with data points at 7.6-m intervals. The terrain was flat enough that no spacing corrections needed to be made. Slingram data are "bifocal" in regard to sensitivity, and, consequently, inhomogeneities near either the transmitter or receiver may have a greater effect than do inhomogeneities in between. Nevertheless, there was no practical way to delineate the exact location of the inhomogeneities. Therefore, the standard practice was followed of plotting the data at the center of wherever the 60-m line was positioned at the time of the reading.

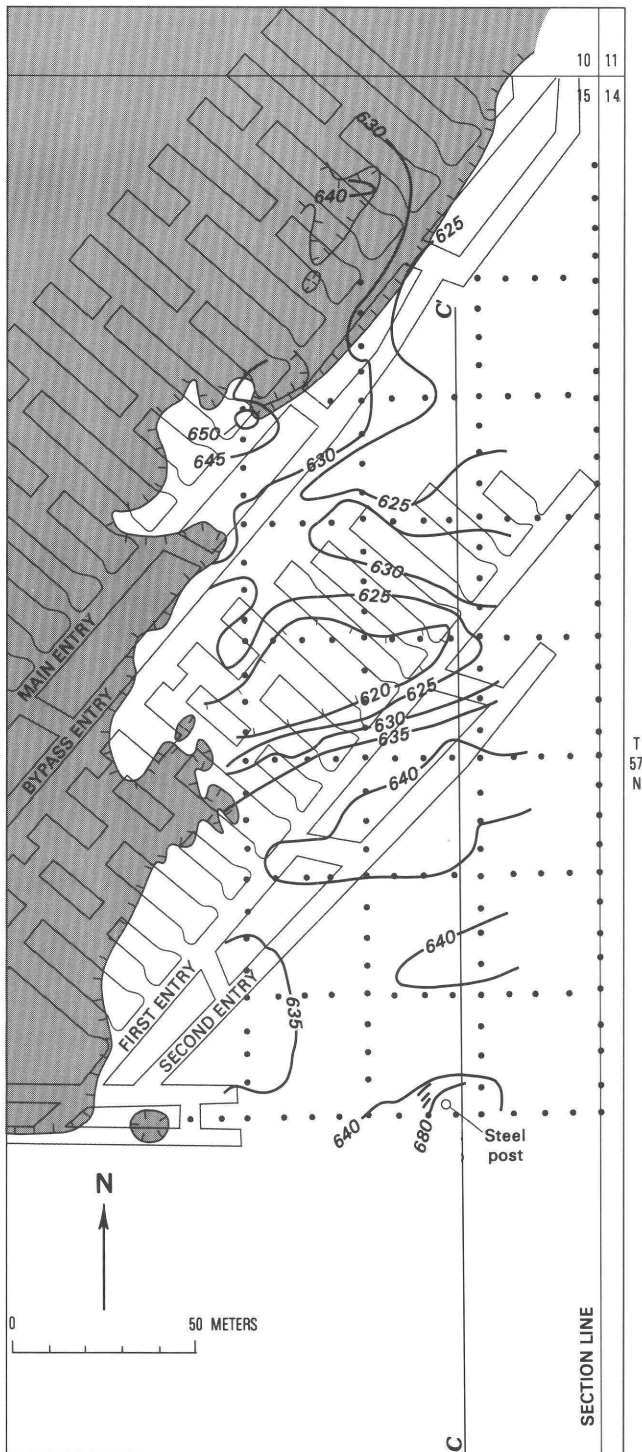
Figures 13 and 14 show the electromagnetic fields in plan view of the three profiles for both the in-phase and out-of-phase components, respectively, of the site 2 survey. The in-phase field is considerably less complex than the out-of-phase field. The in-phase field of figure 13 has a generally broad gradient that increases toward the west and perhaps the north. Low anomalies in the in-phase field include a general low over the northeast end of the second entry of the nonsubsided area and a small unexplained low in the south-central part of the area. The out-of-phase component map (fig. 14) also shows a broad relatively high anomaly over the nonsubsided mine

workings and a low anomaly over the northeast end of the second entry of the nonsubsided area.

A cross section along C-C' (figs. 13, 14) of the electromagnetic components is shown in figure 15. The out-of-phase component shows its lowest anomaly over the second entry of the newer workings. The cause of the anomaly is unknown, but two possibilities seem eminent: (1) metal objects abandoned in the mine and (2) resistivity boundaries, which correspond to mechanical boundaries between disturbed and undisturbed ground.

Computations of electromagnetic fields are complicated, but according to Watts (1978) a long, straight metal conductor, for example, that is buried less than one-fourth skin depths will significantly disturb the ambient electromagnetic fields. Skin depth (the effective depth of penetration of electromagnetic energy in a conducting medium (Sheriff, 1974)) is equal to $(2\rho/\mu\omega)^{1/2}$ where ρ is resistivity, in ohm-meters, μ is magnetic permeability in henries/meter, and ω is angular frequency. One-fourth skin depth was computed for site 2 as a function of resistivity. The relatively low magnetic permeability of the magnetite-bearing sedimentary rocks and coal is only slightly more than free space; it was assumed to be 13×10^{-7} H/m. Angular frequency was obtained from 1,760 Hz, which was the survey frequency.

Resistivities of the sedimentary rocks and coal of the Fort Union Formation at site 2 were not available in the area of the Acme Mine. An indication of representative resistivities in undisturbed ground was available, however, from borehole S-2 (fig. 8B) in the same geologic formation some 13 km south at Sheridan, Wyo., and from borehole B-1 (fig. 8A) in the similar Wasatch Formation some 67 km to the south, at Buffalo, Wyo. The resistivity logs of boreholes B-1 and S-2 of figure 8 both indicate resistivities that range from about 10 to 100 ohm-meters. The clays, shales, and mudstones tend to be responsible for the



R 84 W

EXPLANATION



Magnetic field intensity in gammas—
For total value, add datum of 57,000
gammas; contour hachured to indicate
closed area of lower magnitude; contour
interval 5 or 10 gammas

• Station point

Figure 11. Acme Mine, showing contours of magnetic field of site 2, in relation to passages (mine map, Sheridan, Wyoming Coal Company, 1938), and limits (hachured line) of visible broad surface subsidence (shaded).

lower resistivities; the siltstones and sandstones show intermediate resistivities; and the coals show the higher resistivities.

Skin depth varies with resistivity as well as with frequency. The depth to which one-fourth skin depth is affected by the beds at site 2 is unknown, but the “effective” resistivity at that site is estimated to range from about 10 to 70 ohm-meters. The corresponding range of one-fourth skin depth (fig. 16) is about 10–22 m. This range of depth essentially includes all the possible thicknesses of overburden as well as the workings of the Acme Mine at site 2. It indicates that relatively long, straight metallic conductors might be detected by this electromagnetic survey. Note, however, that these conditions require rails that are connected and not badly rusted—conditions that may not be realistic in the Acme Mine.

An alternative interpretation does not require abandoned metal in the mine. Strong imaginary-component anomalies, such as those indicated in figure 15, are often seen over resistivity boundaries, which in this case would probably correspond to the ground-water variations between disturbed and undisturbed ground.

Gravity Survey and Gravity Field Characteristics

A gravity survey was run over the grid at site 2 using a temperature-compensated precise Worden Master¹ gravity meter. The observed gravity values at the site were referenced to International Gravity Base IGB-15546E at the new Sheridan, Wyo., Post Office (E.J. Hauer, Chief of Department of Defense Gravity Services Division, Defense Mapping Agency, St. Louis Air Force Station, MO 63118, written commun., Aug. 1976), which is 980,228.81 mGal.

A temporary gravity base was also set near the grid of site 2. Traverses of several stations were made at one time from the temporary base, and individual traverses were done in less than an hour. Error of closure was no more than about 0.1 mGal, averaging about 0.07 mGal. Instrumental drift was considered linear and all closure errors were distributed with respect to time to the stations established during the traverse. Each station was read at least three times, or until the scale readings agreed within the equivalent of about 0.005 mGal. The three or more readings were completed within about 2 minutes and a complete traverse was done within about 15 minutes. The individual traverses were also tied together by repeating individual stations.

Simple Bouguer values were reduced to sea level and were computed for each of the gravity stations over site 2 by adding the observed gravity and elevation

¹The use of trade names is for descriptive purposes only and does not constitute endorsement by the U.S. Geological Survey.

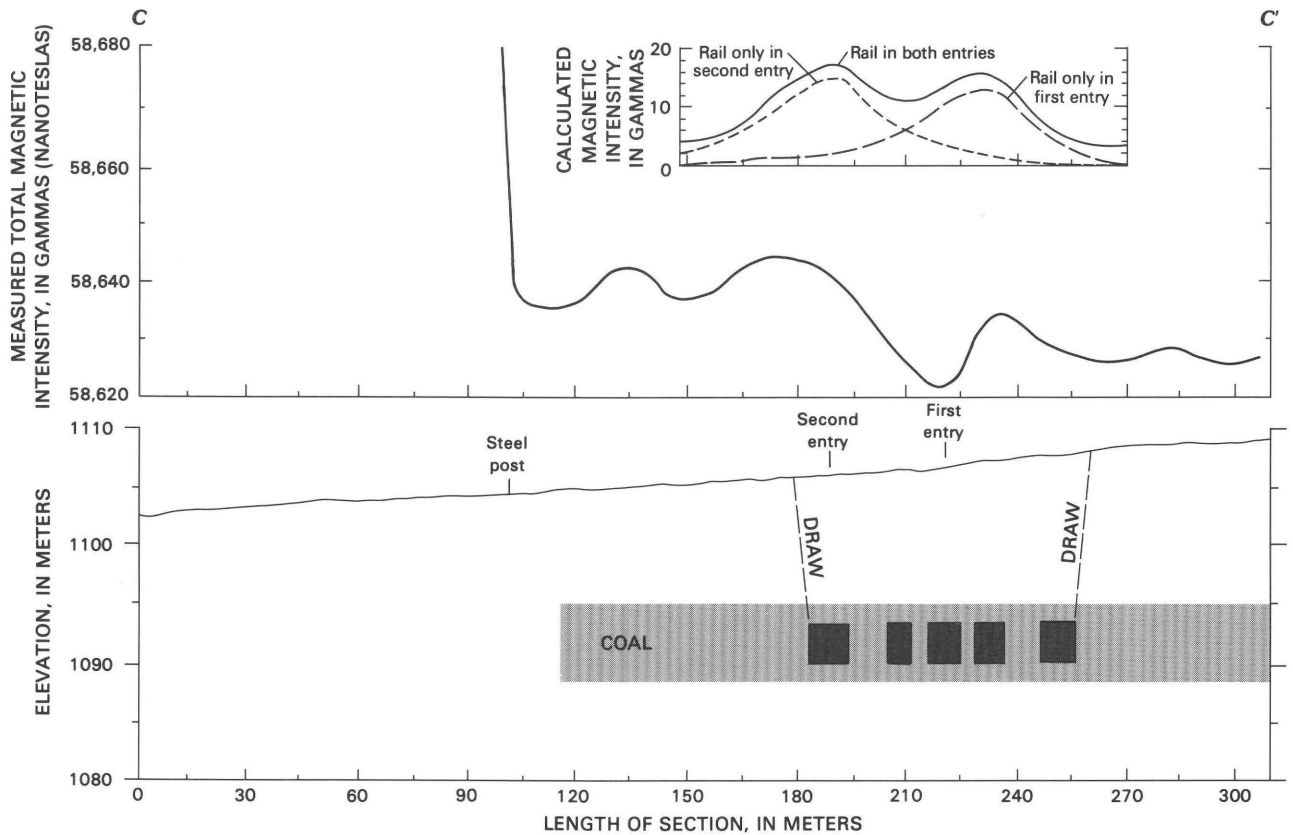


Figure 12. Magnetic anomalies calculated for mine-car rails in first and second entries and along cross section C-C' (fig. 11) of site 2 and compared to measured magnetic field. Draw lines are theoretical limits of subsidence; mine openings are estimated.

correction and subtracting the latitude correction. Only simple Bouguer values were computed because the topography of site 2 is very flat and all terrain corrections within a few hundred meters of each station would be approximately the same. There may be a relatively broad regional effect in the gravity field, however, because of the higher topography north of the grid.

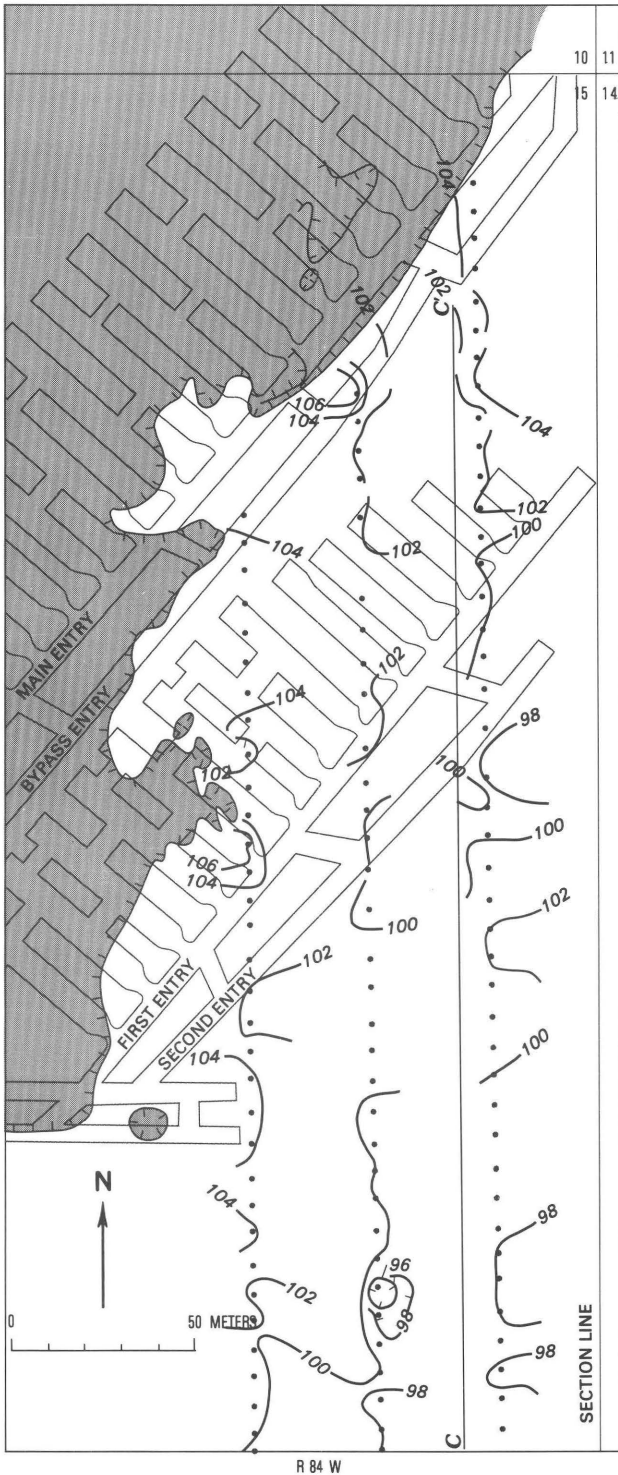
Elevation corrections (combined Free Air and Bouguer corrections) of 2.67, 2.00, and 1.70 g/cm³, corresponding to crustal densities above sea level, were applied. Latitude corrections were applied using the international gravity formula: $g = 978031.85(1 + 0.005278895 \sin^2\phi + 0.000023462 \sin^4\phi)$ mGal (E.J. Hauer, written commun., 1976).

Possible error in the simple Bouguer survey is attributed to error in determination of station elevations and to measurement inaccuracy with the gravity meter. The elevations of the grid were leveled to an accuracy of about 0.015 m, as mentioned previously, which corresponds to an error in the simple Bouguer anomaly of about 0.003 mGal. Inaccuracies in the horizontal positioning of the survey are negligible. Accuracy of reading the gravity meter is about 0.005 mGal, and errors due to an assumption of linear drift in the meter and in small

Earth-tide variations are estimated to be no more than a few thousandths of milligals. Total accuracy of the simple Bouguer anomalies is, therefore, within about 0.015 mGal.

Densities of the sedimentary rocks and coal of the Fort Union Formation were not available from the Acme Mine. Representative core densities were available, however, from the S-2 borehole (Farrow, 1980) in the Fort Union, the formation that contains the Acme Mine. The densities are plotted in figure 8 along with the lithologic log of the borehole. Twenty-six densities of mainly sedimentary rocks average 2.3 g/cm³. Coal densities are not well represented, however, because the cores disintegrate easily. The density of subbituminous coal is somewhat lower than that of the sedimentary rocks (Farrow, 1976).

Three simple Bouguer gravity maps were prepared for site 2 using densities for the Bouguer corrections in the data reductions of 1.70 g/cm³ (fig. 17), 2.00 g/cm³ (fig. 18), and 2.67 g/cm³ (fig. 19). There is no strong contour pattern that suggests that the mine openings control the simple Bouguer gravity field. On the contrary, each of the three contour maps shows a broad gravity high over the nonsubsided mined area and general gravity



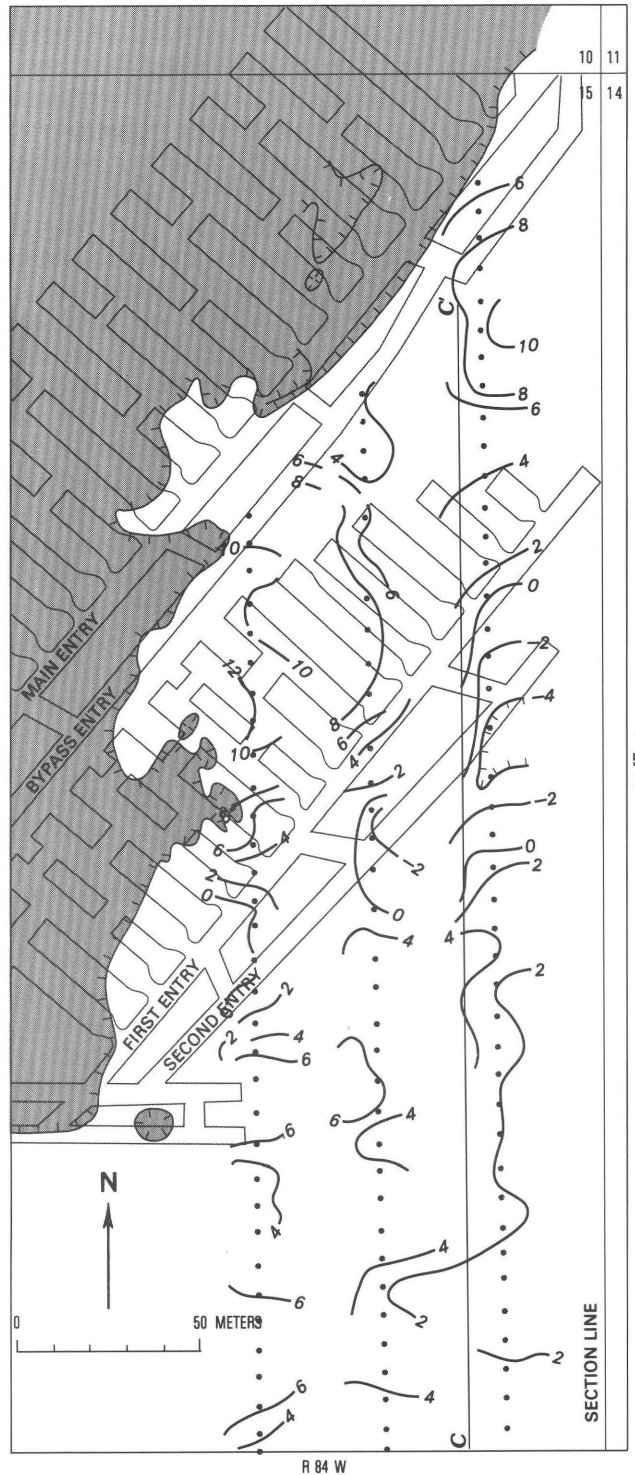
EXPLANATION



Electromagnetic contour—Showing in-phase component, referenced to 100 percent; hachured to indicate area of low magnitude

• Survey point

Figure 13. Electromagnetic field (Slingram) of site 2, in-phase component; input frequency is 1,760 Hz and there is 60-m separation between transmitter and receiver. Shown in relation to passages and to limits (hachured line) of visible broad surface subsidence (shaded).



EXPLANATION



Electromagnetic contour—Showing out-of-phase component, referenced to 0 percent; hachured to indicate area of low magnitude

• Survey point

Figure 14. Electromagnetic field (Slingram) of site 2; out-of-phase component; input frequency is 1,760 Hz and there is 60-m separation between transmitter and receiver. Shown in relation to passages and to limits (hachured line) of visible broad surface subsidence (shaded).

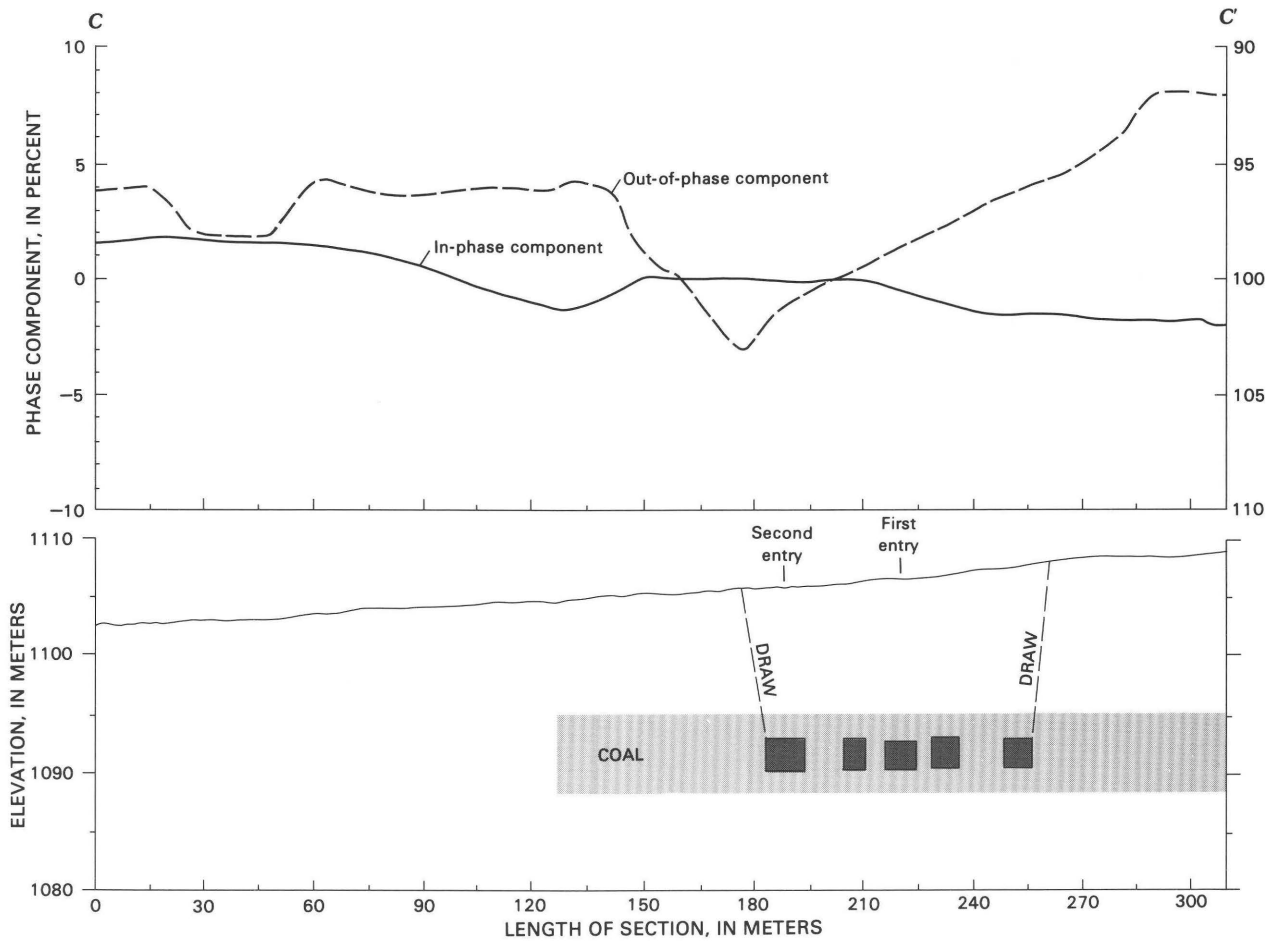


Figure 15. In-phase and out-of-phase electromagnetic components along cross section C-C' of site 2 (figs. 13 and 14).

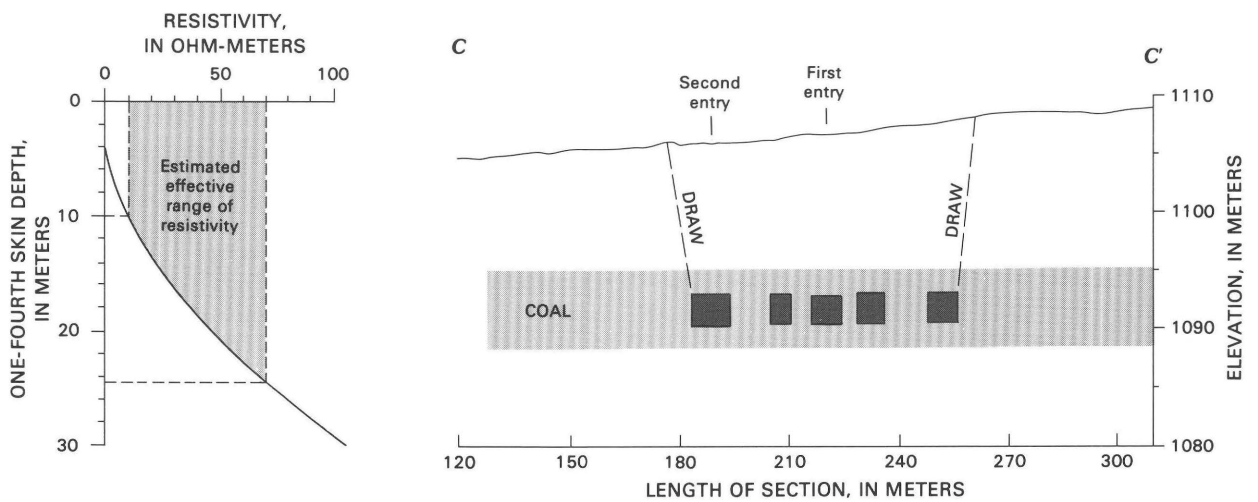
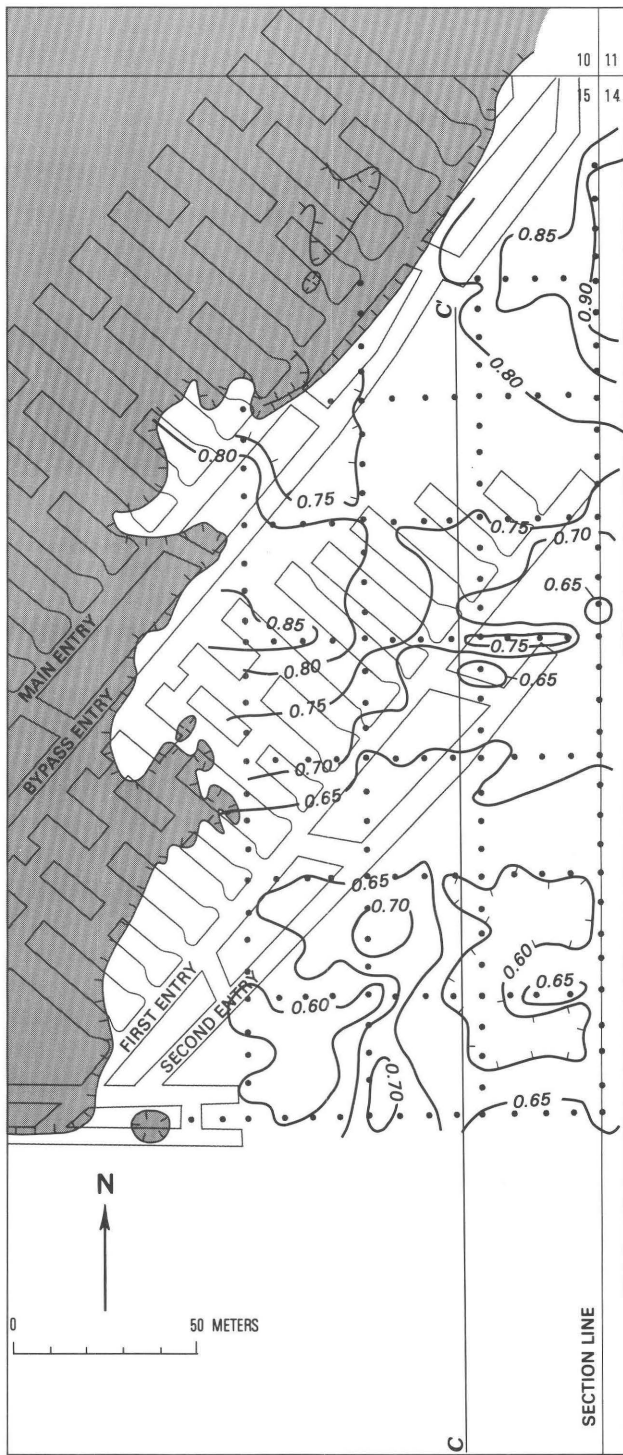


Figure 16. Calculated effective depth of resolution for one-fourth skin depth of penetration for an electromagnetic source as a function of resistivity (10–70 ohm-meters) along cross section C-C'. Input frequency is 1,760 Hz and magnetic permeability is 13×10^{-7} H/m.



R 84 W

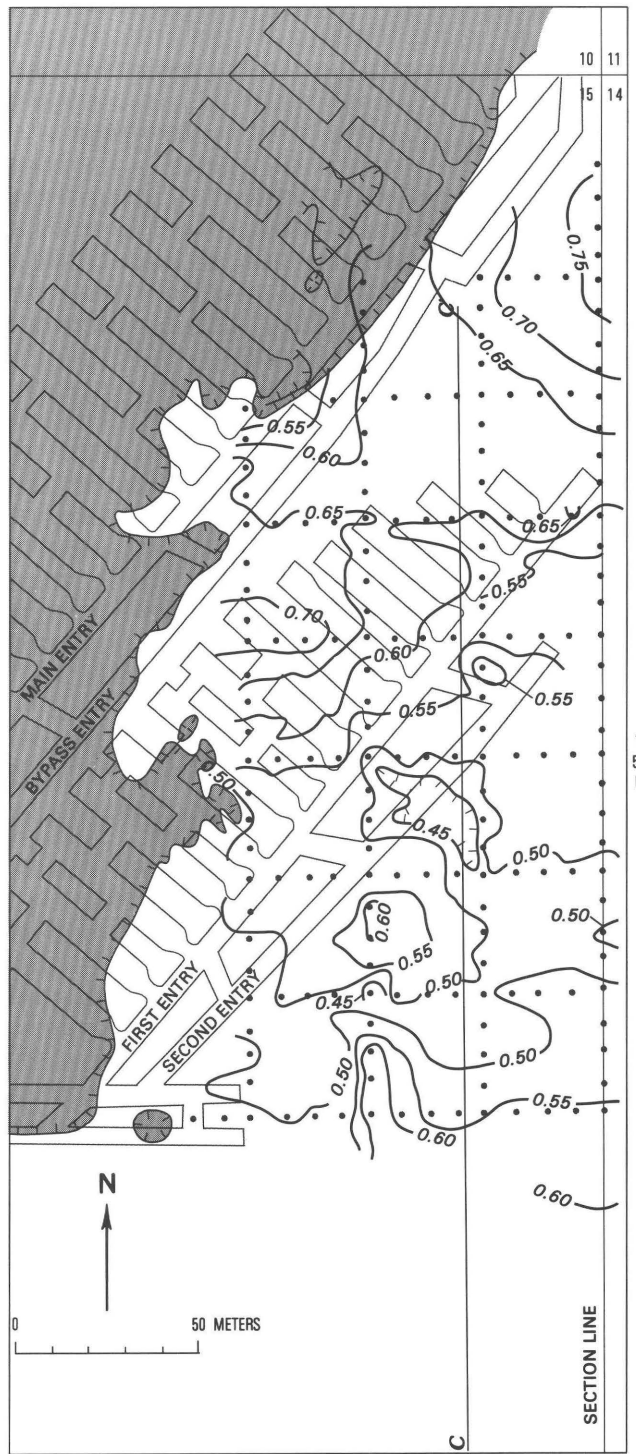
EXPLANATION

Gravity contour—Shown in milligals; add -107 mGal for simple Bouguer gravity anomaly; hachured to indicate area of low magnitude. Contour interval 0.05 mGal

• Survey point



Figure 17. Simple Bouguer gravity field of site 2, reduced at a density of 1.70 g/cm³. Shown in relation to passages and to limits (hachured line) of visible broad surface deformation (shaded).



R 84 W

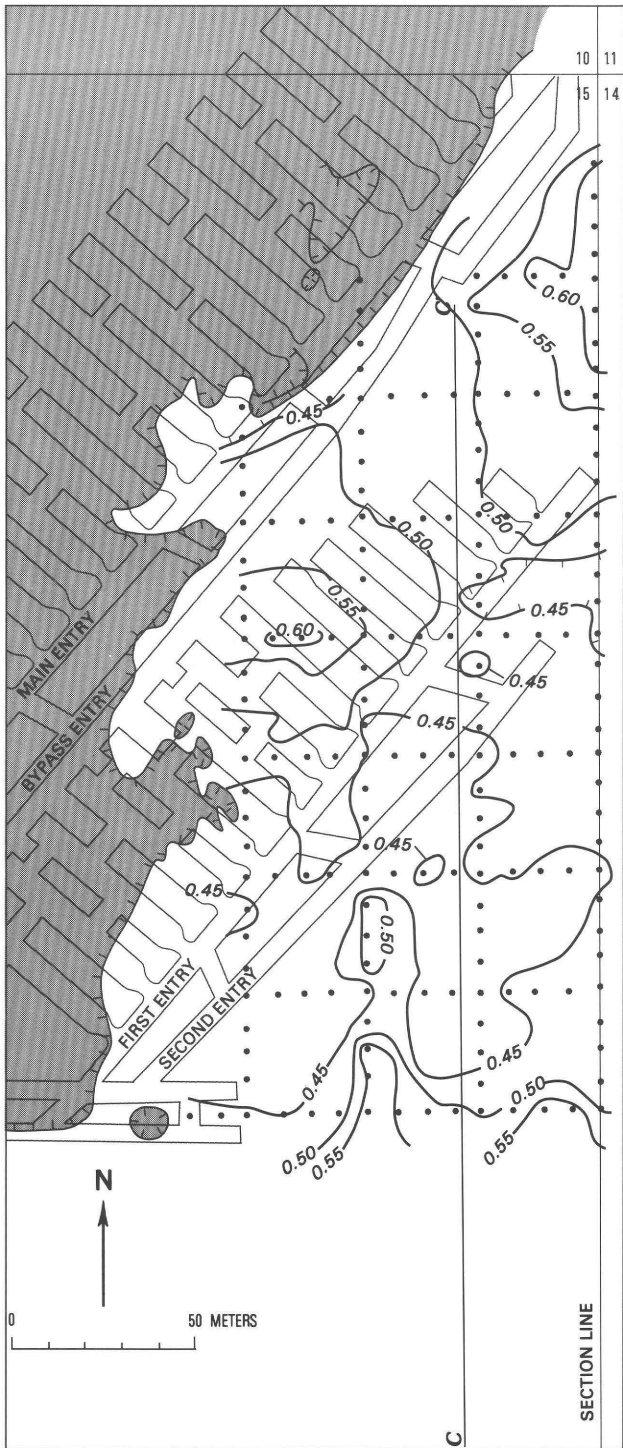
EXPLANATION

Gravity contour—Shown in milligals; add -121 mGal for simple Bouguer gravity anomaly; contour hachured to indicate closed area of lower magnitude. Contour interval 0.05 mGal

• Survey point



Figure 18. Simple Bouguer gravity field of site 2, reduced at a density of 2.00 g/cm³. Shown in relation to passages and to limits (hachured line) of visible broad surface subsidence (shaded).



EXPLANATION

• Survey point

○ 0.50 Gravity contour—Shown in milligals; add -147 mGal for simple Bouguer gravity anomaly; contour hatched to indicate closed area of lower magnitude. Contour interval 0.05 mGal

Figure 19. Simple Bouguer gravity field of site 2, reduced at a density of 2.67 g/cm^3 . Shown in relation to passages and to limits (hatched line) of visible broad surface deformation (shaded).

lows along the southeast side but away from the mined area. An anomaly with an amplitude of less than 0.1 mGal and of relatively small areal extent occurs over the most northeasterly crosscut between the first and second entries.

Figure 20 shows theoretical two-dimensional gravity anomalies caused by the mine openings compared to the measured simple Bouguer gravity anomalies slightly west of cross section $C-C'$ (figs. 17, 18, 19). The mine openings to the north of cross section $C-C'$ also were considered for the theoretical computations, and the gravity anomalies due to any mine openings were assumed to extend several times their width at right angles to the cross section. Theoretical gravity anomalies were computed for both air- and water-filled mine workings with a rock density of 2.30 g/cm^3 . The regional gradient was assumed to be flat.

The measured simple Bouguer profiles along $C-C'$ show a broad low anomaly south of the nonsubsided part of the mine, instead of over it, and a broad high anomaly over the entries, increasing in magnitude to the north. The reason for these anomalies is unclear; perhaps there are broad lateral changes in the densities of the underlying sedimentary rocks. The cause of the anomaly of small areal extent over the crosscut between the first and second entries is likewise unknown. The anomaly is actually composed of a relatively low portion on the south and a high portion on the north. The low portion could be caused by a relatively near surface cavity caused by upward stoping during subsidence, but the high portion must have another cause. Either portion could be caused by error or a relatively rapid lateral change in near-surface density.

Both the water- and air-filled profiles of the theoretical gravity anomalies are lowest north of the newly mined area because of the influence of the subsided mines on the north. The computed gravity profile exhibits a maximum amplitude of about 0.4 mGal for the water-filled mine and about 0.9 mGal for the air-filled mine—both considerably greater than the estimated possible error in the gravity survey of 0.015 mGal . However, neither computed gravity profile is similar in configuration to the measured gravity along profile $C-C'$.

Seismic Survey

Seismic-refraction surveys were run over the non-subsided portion of the mine at site 2 (fig. 2). Background information for the interpretation of these surveys in site 2 was provided by (1) some in-hole seismic measurements done by Birdwell, Inc., Tulsa, Okla., on rocks of similar composition as those at the mine along with seismic-refraction measurements along the ground surface near the boreholes and (2) some seismic-refraction measurements over a soil arch that bridged subsided bedrock and coal.

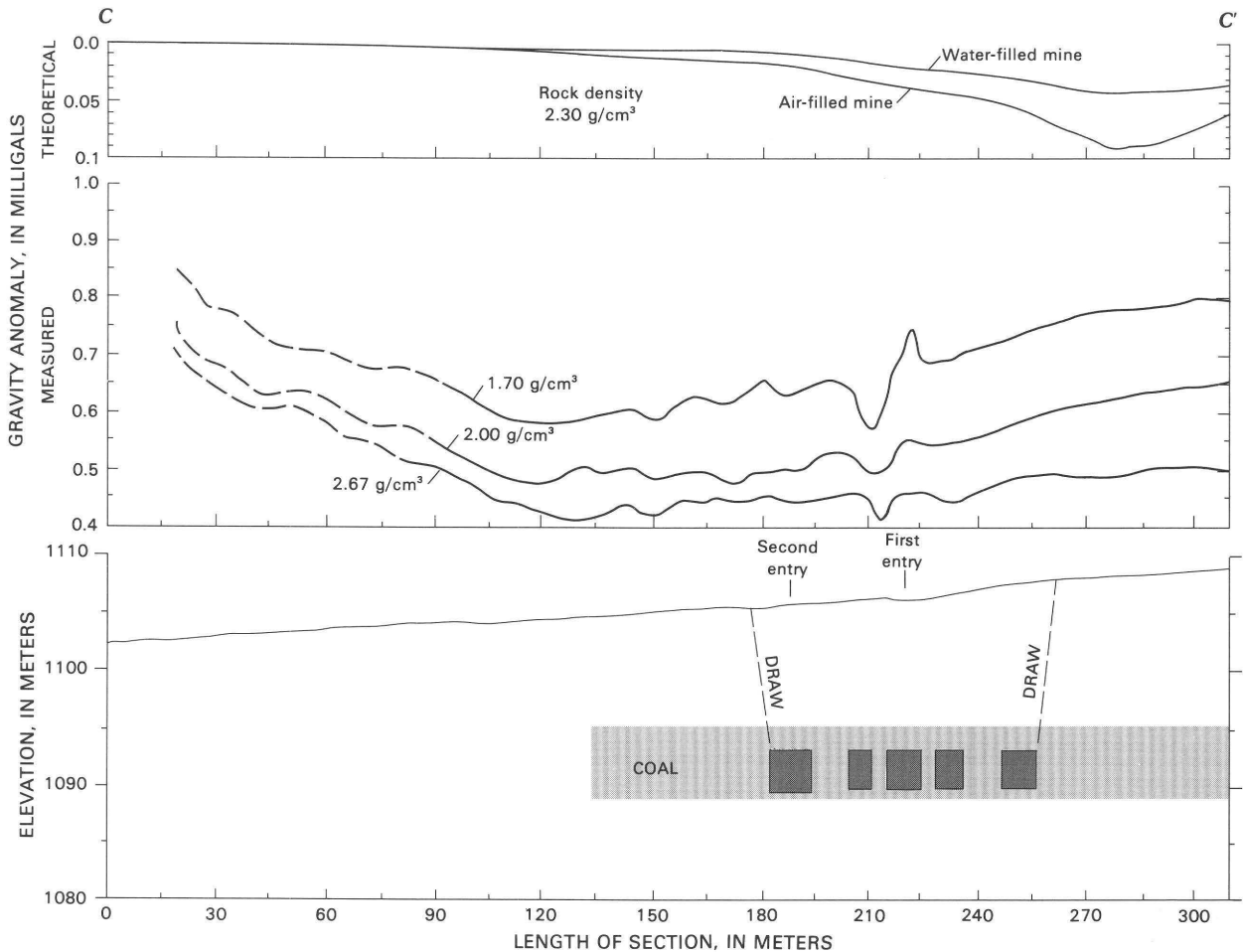


Figure 20. Simple Bouguer gravity anomalies along C-C' for data reduced at three densities (1.70 g/cm^3 , 2.00 g/cm^3 , and 2.67 g/cm^3) compared with theoretical gravity anomalies computed for both air- and water-filled mine openings. Draw lines are theoretical limits of subsidence; mine openings are estimated.

Figure 8 shows velocity data interpreted from depth versus velocity for two boreholes for both downhole and surface-run surveys. Borehole S-2 (fig. 8B; Farrow, 1980) was cored into the Fort Union Formation, which also includes the coal and rocks of the Acme Mine, and borehole B-1 (fig. 8A; Farrow, 1976) was cored into the Wasatch Formation. Although S-2 and B-1 are distant from the Acme Mine and from each other, they are cored in similar lithologies, and their measured velocities are very similar. Because the lithology of these two boreholes is quite similar to that of the undisturbed ground of site 2, it follows that their velocity data may also be indicative of those at site 2.

The seismic measurements at boreholes S-2 and B-1 show a low-velocity layer that overlies a high-velocity layer. The low-velocity layer is defined by the first segment of the time-distance graphs; its seismic velocity ranges from about 360 to 480 m/s and its thickness from about 2.4 to 5 m. The underlying high-velocity layer is defined by both the segment of the time-distance graphs

and by the in-hole velocity graphs. The seismic velocity of the high-velocity layer exceeds 1,520 m/s and is infinitely thick for the purposes of this study.

The in-hole velocities of figures 8A and B were interpreted from sonic logs that were run within 12 m of the ground surface. Therefore, measurements were taken only in the bedrock (high-velocity layer). The in-hole velocities of both boreholes S-2 and B-1 were best-least-square fitted for both linear and logarithmic functions of depth. The best fit for the velocities of each hole is probably the logarithmic curve, but the velocity gradients of the linear fits are more easily compared; these are 3.7 m/s/m of depth in borehole S-2 and 3.4 m/s/m in borehole B-1.

Most seismic-refraction lines run for engineering purposes elsewhere in the northern Powder River Basin indicate a correlation between the low-velocity layer and undivided weathered bedrock and overlying surficial deposits. On the other hand, the high-velocity layer is characteristic of nonweathered sedimentary bedrock of either the Fort Union or Wasatch Formation.

Although borehole velocity data were not available at the Acme sites, a comparison between the surface-run velocities at boreholes S-2 and B-1 and elsewhere in the Powder River Basin shows that, within broad limits, either the bedrock or overburden can be identified from velocity data.

Soil Arch (Site 1) as Model

Subsidence in at least one place in site 1 created a soil arch that can be visually verified (fig. 21). The arch is at least 7 m in vertical thickness at its center and apparently is developed only in the mantle of soil and not in the underlying bedrock. The bedrock has apparently stoped and raveled, and the loose debris has migrated into the mine openings below. Seismic line 1 of figure 21 was run directly over the bridge and seismic line 2 was run nearby, where other near-surface underground openings also apparently existed (fig. 2).

The time-distance curves for seismic lines 1 and 2 across the soil arch of site 1 are also included in figure 21 for 11 geophones with spacings of 3.35 m. An explosive energy source was used on line 1 and repeated sledgehammer blows were used on line 2 as energy sources in conjunction with a signal-enhancing seismograph. Record quality was good. The low-velocity segments of these graphs range from 350 to 580 m/s, which is close to the range of low-velocity segments of 347 to 475 m/s measured at boreholes B-1 and S-2 (fig. 8). A second segment with higher velocity than the low-velocity segments is shown on each time-distance graph in figure 21 for site 1. These second segments do not represent seismic velocities for bedrock because (1) the second segment velocities are far less than those bedrock velocities measured in boreholes S-2 and B-1, (2) the seismic lines are not long enough to exceed the critical distance required by the thickness of the soil, and (3) the second segments indicate atypical data that are probably caused by deformation in the soil.

Seismic Field of Site 2

Figure 22 shows five seismic-refraction lines along two traverses in plan view that were run in site 2. The lines are each about 100.5 m long with geophone spacings of 9.1 m. Adjacent lines overlap by about 10 m. The energy sources for the resulting seismograms were the equivalents of about three-quarter-pound charges of dynamite. They were detonated at depths of about 1.5 m in boreholes. Record quality was very good.

Figures 23 and 24 show the time-distance graphs as well as the velocity layering at depth along cross sections $D-D'$ and $E-E'$ (fig. 22) for the five seismic lines. The velocities of the V_{p1} segments of the graphs range

from 340 to 520 m/s, averaging about 400 m/s; the velocities of the V_{p2} segments range from 1,830 to 2,870 m/s. The V_{p2} segments of those lines over the mined area have a marked tendency to be nonlinear, whereas those lines away from the mined area tend to be more linear. The V_{p2} segments that are apparently affected by the mining include all of lines 3, 4, and 5. Those lines that are seemingly not affected include line 1 and possibly line 2.

The depth and configuration of the $V_{p1}-V_{p2}$ interface were computed by the method of differences for a two-layer case (Laby, 1931; J. C. Hollister, written commun., 1957; Redpath, 1973). This method of computing accommodates the variable thickness of the low-velocity layer. These variations may be due to changes in the surface topography and (or) in the topography of the buried contact between the low-velocity and high-velocity layers. There is little topographic relief at the ground surface along cross sections $D-D'$ and $E-E'$, however, nor does the $V_{p1}-V_{p2}$ interface change elevation very rapidly. The very irregular velocity segments, therefore, seem to be attributable to the mining and subsidence.

Most seismic-refraction lines run for engineering purposes elsewhere in the northern Powder River Basin indicate a correlation between the V_{p1} layer and surficial deposits (alluvium, colluvium, eolian deposits, etc.) and between the V_{p2} layer and bedrock of the Tertiary, Wasatch, and Fort Union Formations (Miller, 1979). The thicknesses of these V_{p1} (low-velocity) layers are as great as 12 m, but 3-6 m is more typical. The thicknesses of surficial deposits along lines $D-D'$ and $E-E'$ are unknown, but bedrock is exposed at depths of less than 4 m in the subsidence pits just west of line 4 (fig. 22). The equivalent depths to the apparent $V_{p1}-V_{p2}$ interface are as much as 10-12 m. Because the depth to the apparent $V_{p1}-V_{p2}$ interface along $D-D'$ and $E-E'$ is as much as twice that of the nearby surficial deposits or even that of most other measured surficial deposits across the Powder River Basin, we suspect that the low-velocity layer (V_{p1}) may be apparently thickened by deformation in the bedrock above the mine.

Seismic-refraction theory requires that the part of a refracted wave that travels in the V_{p2} layer and that contributes to the first arrivals at the seismometers will travel just below the $V_{p1}-V_{p2}$ interface. Velocities measured in the bedrock of the Fort Union and Wasatch Formations, however, increase with depth (fig. 8). The average linear increase of velocity with depth of boreholes B-1 and S-2 is about 3.6 m/s/m of depth. Figure 25 demonstrates the theoretical travel path in a medium of two layers: V_{p1} (overburden) is 400 m/s, does not increase with depth, and has a thickness of 10 m; V_{p2} (bedrock) is 2100 m/s just under the interface, increases with depth, and has infinite thickness. The V_{p2} segment of the time-distance graph is hyperbolic and imperceptibly

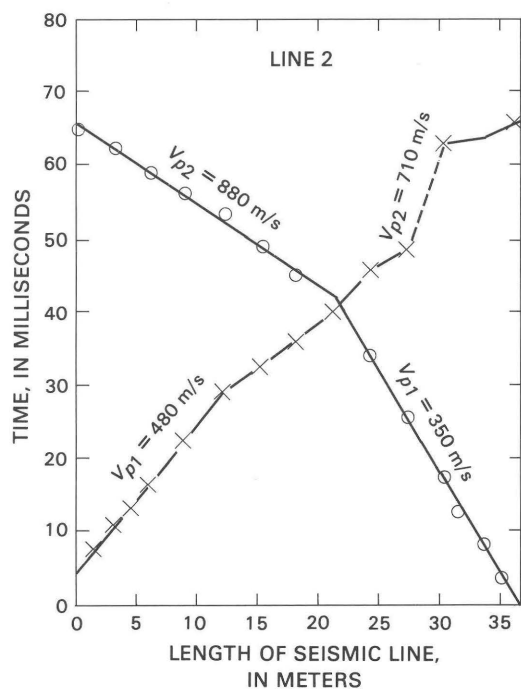
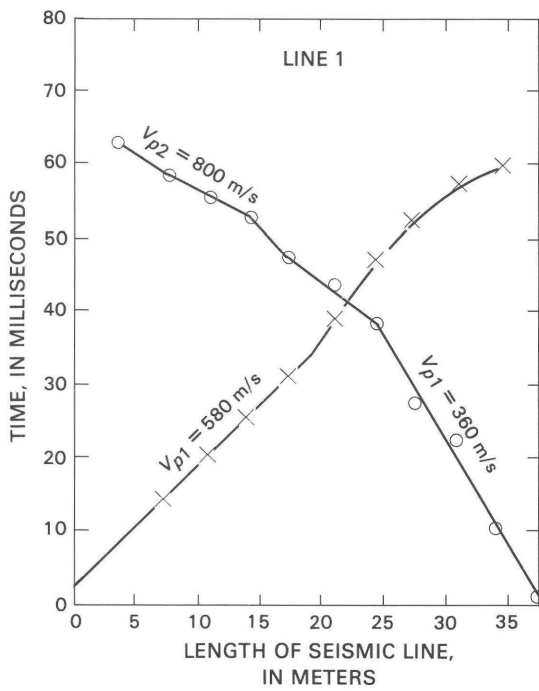
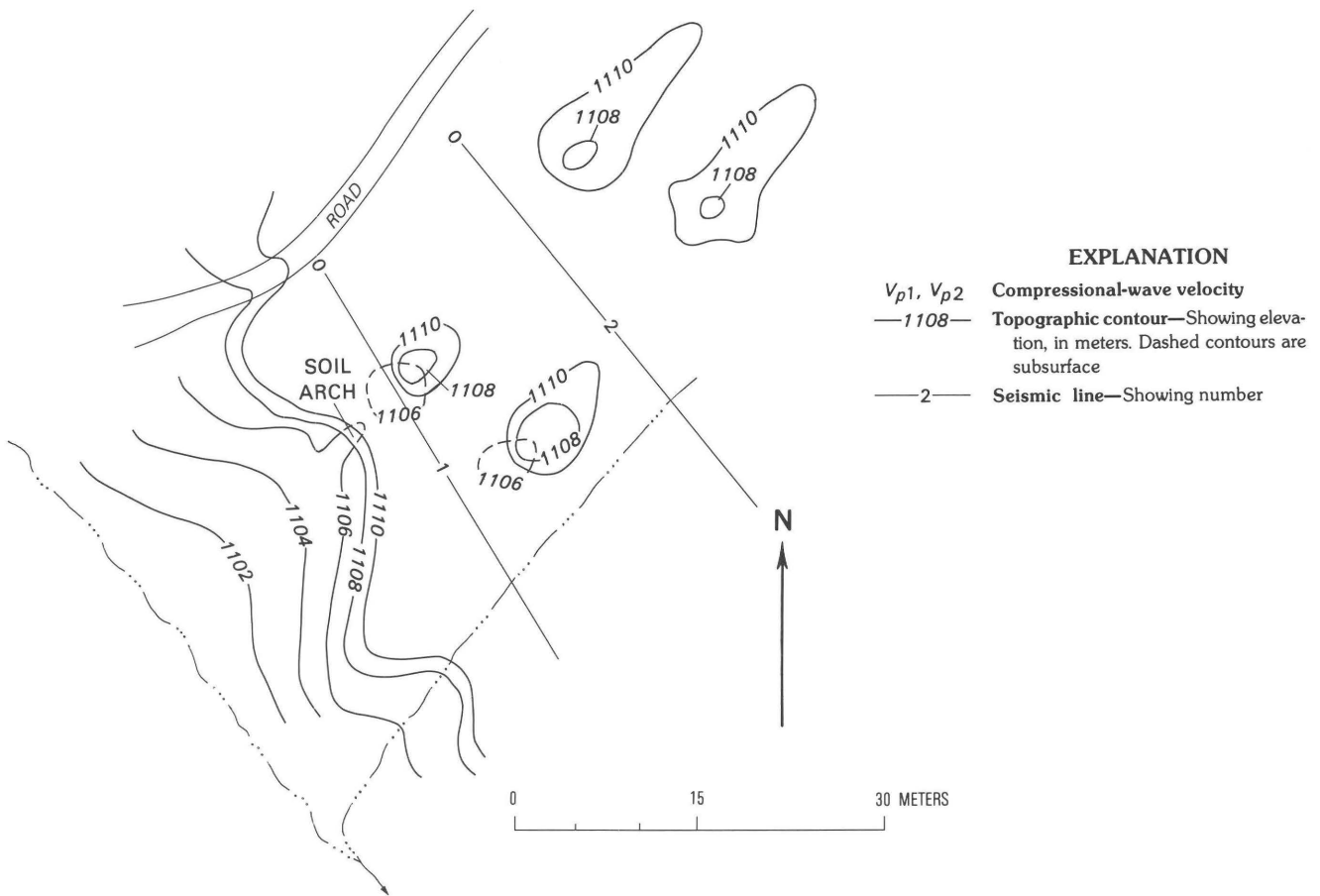
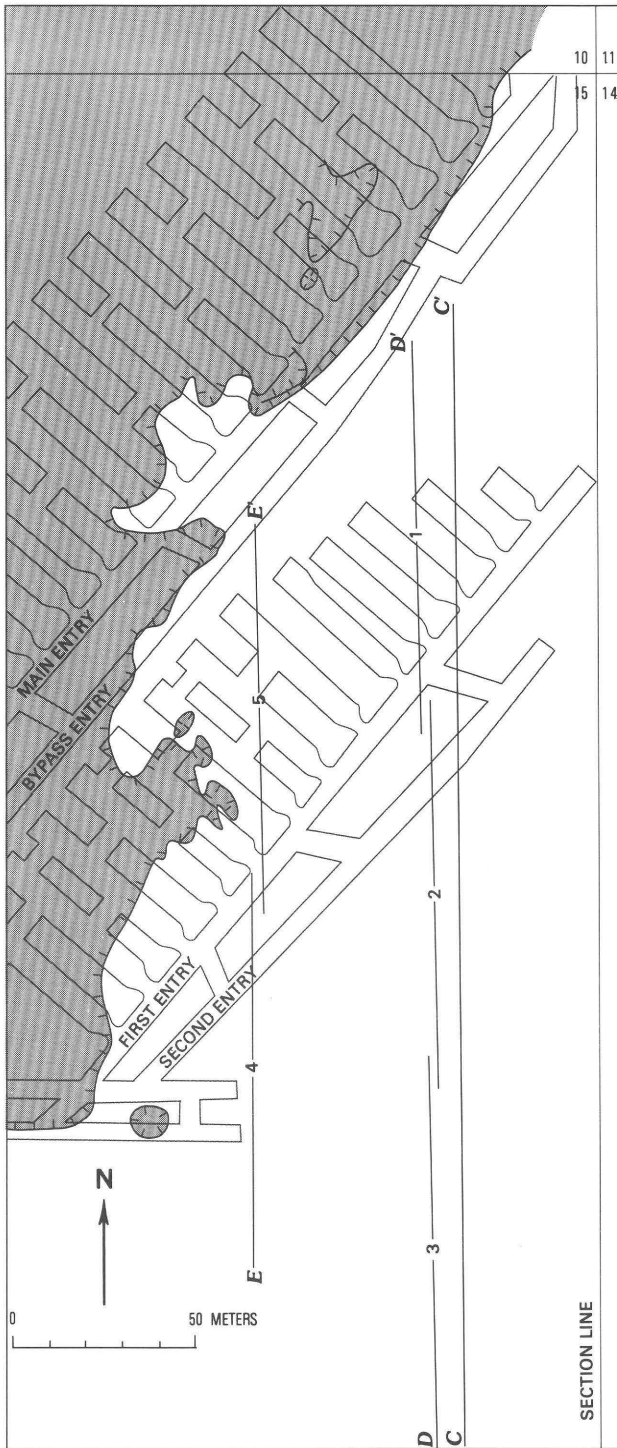


Figure 21. Map of a soil arch in site 1 showing topography, location of seismic lines, and time-distance graphs.



EXPLANATION

— 4 — Seismic line and number

Figure 22. Location of seismic-refraction lines 1-5 along D-D' and E-E' at site 2. Shown in relation to passages and to limits (hachured line) of visible broad surface deformation (shaded).

concave downward. The wave paths are linear in the V_{p1} layer and segments of circles in the V_{p2} layer (Ewing and Leet, 1932). Curvature along the hyperbolic segment in the graph is so slight for the 200 m or so shown in figure 25 that it cannot be detected by eye. Because of this very slight curvature, straight-line segments commonly are made instead of curves in time-distance graphs for the V_{p2} segment (Palmer, 1983).

Theoretical travel paths in the V_{p2} layer are shown in figure 25 for horizontal intervals of approximately 50 m to about 200 m. The maximum depth of penetration for seismic waves along a seismometer line of about the same length as those run in site 2 (105 m) is only about 2.3 m into "bedrock." By analogy, the first arrival times on the time-distance graphs of lines 1-5 are contributed by wave fronts that do not penetrate as deep as the mine roof of average depth of burial shown in figures 23 and 24, nor even as deep as the mine roof with the least overburden. Therefore, the V_{p2} segments of those seismic lines that are affected by the mines may be caused by deformation in the bedrock above the mine drifts.

SUMMARY AND CONCLUSIONS

One potential hazard in underground coal mining areas in the Powder River Basin, as well as in other parts of the United States, is abandoned coal mines. These mines are hazardous because they may subside and cause damage to the landscape or structures, and the mines may spontaneously ignite and pollute air and water. A further problem with abandoned underground mines is that adequate maps of the underground openings are not always available; hence, the location of some mines may be unknown to local residents until the mines are manifested by surface subsidence. Ways of detecting abandoned but nonsubsided mines are, therefore, very useful and important, and geophysical techniques may offer some solutions.

The Acme Mine was begun in 1911 and abandoned in 1940. Coal was mined by the room-and-pillar method from a coal bed, which is about 6 m thick and with overburden thickness at two geophysical sites estimated to be less than 12-20 m. The surface above much of the mine has subsided and left broad topographic depressions, some of which span many rooms, entries, and pillars.

Two sites that were nearly free of man-made disturbances were chosen for the geophysical surveys over the Acme Mine. Site 1 was selected for a magnetic survey for two main reasons. There is a reasonable chance that abandoned iron is located there. Also, there exists the possibility that heat from the burning mine magnetized the subsidence fractures that extend over most of that site. Site 2 was selected because it had not subsided and the relatively low topographic relief permitted gravity, seismic,

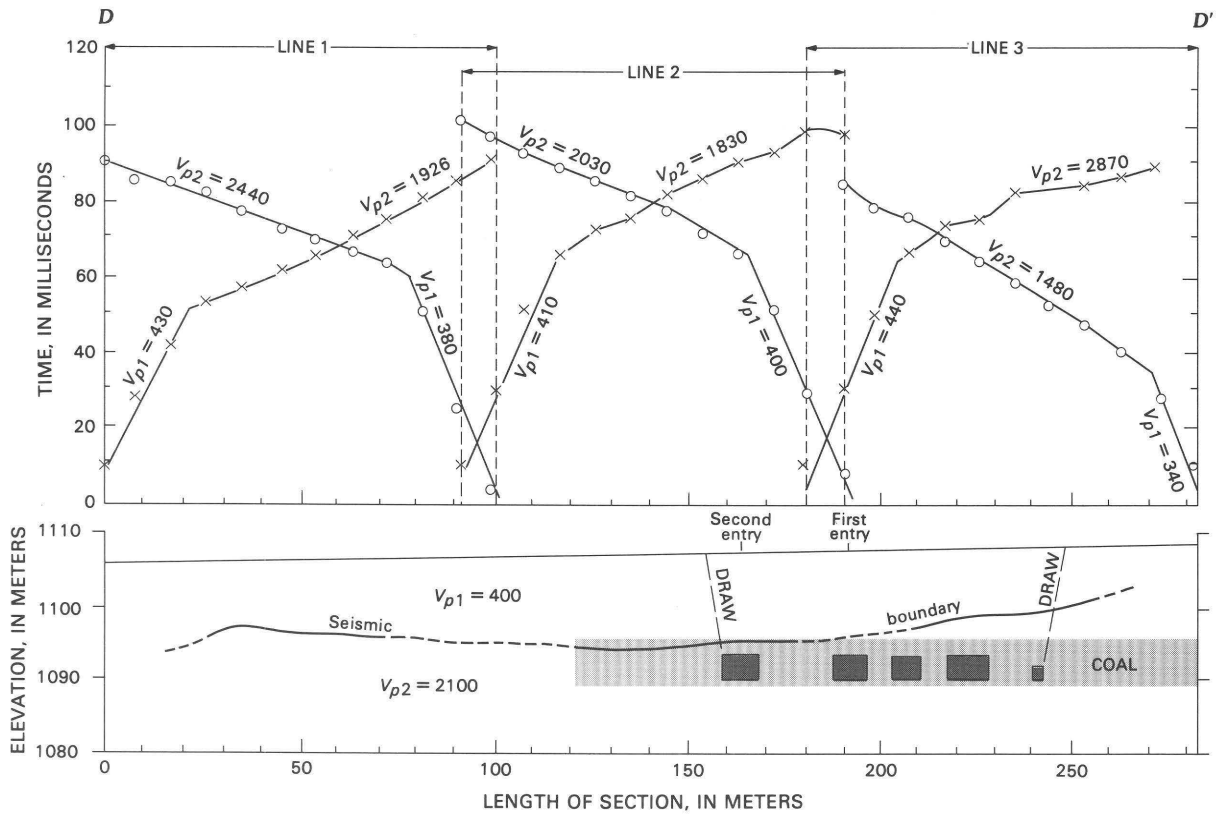


Figure 23. Time-distance curves and velocity-layering interpretation along seismic lines 1-3 (cross section $D-D'$; fig. 22) of site 2. V_{p1} and V_{p2} are compressional-wave velocity in meters per second; x , o , arrival times; dashed line interval, inferred velocity layering.

and electromagnetic surveys, which are sensitive to topographic relief, to be carried out unimpeded. Site 2 also allowed a comparison of the geophysical data obtained over the mine with data obtained away from the mine.

None of the methods employed at Acme Mine adequately located the mine, although some of them hinted at detection. At site 1, the magnetic surveys could positively identify the buried contact of clinkers, which are highly magnetic, and coal that had been mined and the mined portion that had subsided. The magnetic surveys could also positively identify iron-bearing objects that had been dumped into some subsidence pits at site 1 and backfilled with soil. Neither the magnetic nor electromagnetic surveys indicated that any iron-bearing objects such as rails, tools in quantity, or mine cars had been abandoned in the mine at site 2. The electromagnetic surveys indicated the general boundary between the mined and nonmined ground; these electromagnetic indications may have been caused by a higher water content in the bulked material over the mine. The seismic refraction surveys indicated irregular and atypical second-layer velocity segments over both a visible soil arch at site 1 and the nonsubsided mine at site 2; these irregular segments may have been caused by deformation in the

overburden above the mine. Not only did the gravity survey fail to delineate the mine, it also detected a broad high anomaly rather than the expected low situated over the mined area. One speculation for this discrepancy is that the deformed overburden may be more dense, and hence cause greater gravity values because bulking in the overburden may have created greater porosity with consequent water content increase.

The studies have some value in further research. Although the surveys with interpretations were done systematically and with great care, they were largely unsuccessful and, hence, need not be duplicated. However, variations of these survey techniques may be fruitful. A closer spacing of measurement points might be helpful, for example, for all the surveys. The seismic-refraction lines might be restructured so that more lateral information can be ascertained and deep penetration can be obtained. Tidal corrections to increase the accuracy of the gravity survey and electromagnetic equipment that operated at 400 Hz would, of course, be helpful.

Other relatively inexpensive geophysical techniques also can be applied to detecting underground coal mines. Such techniques include the application of shallow seismic reflection or even ground-run radar for very shallow targets.

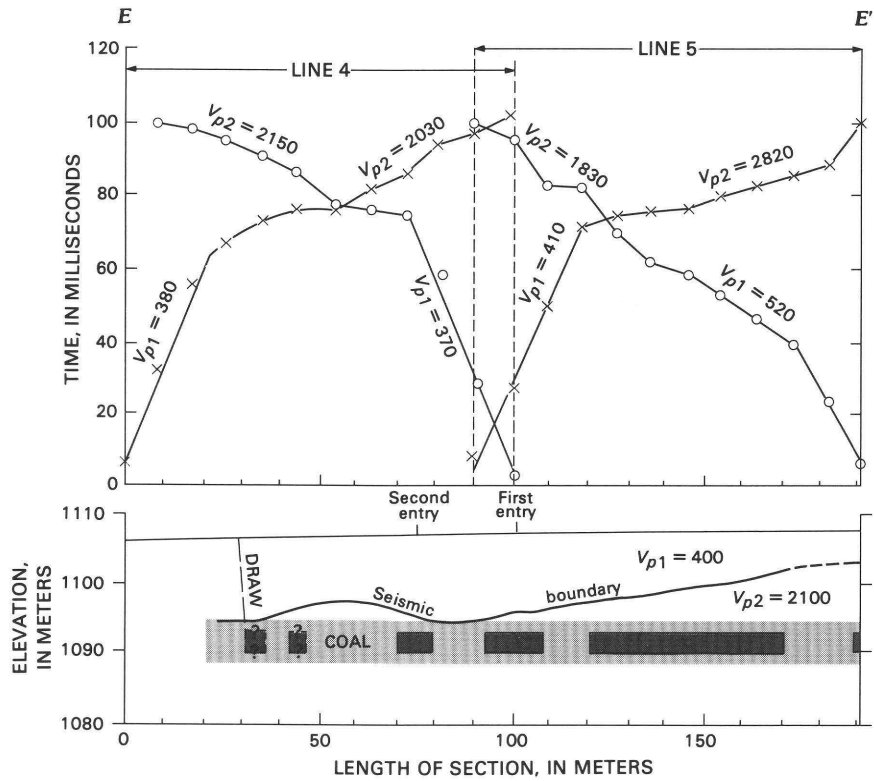


Figure 24. Time-distance curves and velocity-layering interpretation along seismic lines 4-5 (cross section E-E', fig. 22) of site 2. V_{p1} and V_{p2} are compressional-wave velocity in meters per second; x, o, arrival times.

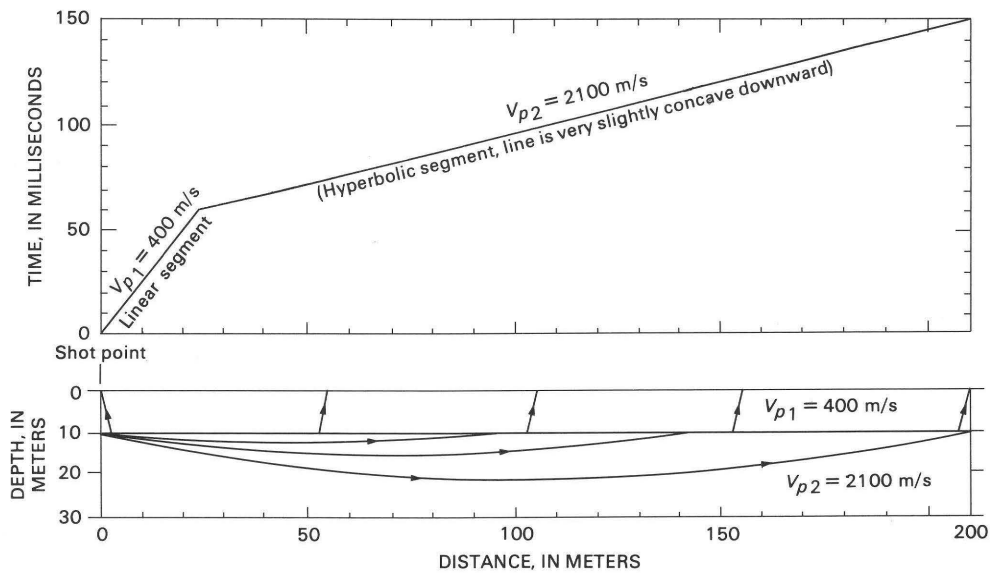


Figure 25. Time-distance graph and theoretical depth of penetration of a seismic wave through a 10-m-thick low-velocity (400 m/s) layer and refracted into a layer of initial velocity 2,100 m/s, which increases linearly with depth at a rate of 3.6 m/s/m.

REFERENCES CITED

- Association of Engineering Geologists, 1978, Seminar on coal mining activities and concepts of multiple land use, selected papers: Association of Engineering Geologists Bulletin, v. 15, no. 2, p. 145-251.
- Bauer, L.P., 1972, The alteration of sedimentary rocks due to burning coal in the Powder River Basin, Campbell County, Wyoming: Texas Technical University M.S. thesis, 65 p.
- Briener, Sheldon, 1973, Applications manual for portable magnetometers: Geometrics, Sunnyvale, Calif., 62 p.
- Dunrud, C.R., and Osterwald, F.W., 1980, Effects of coal mine subsidence in the western Powder River Basin, Wyoming: U.S. Geological Survey Professional Paper 1164, 49 p.
- Ewing, W.M., and Leet, L.D., 1932, Seismic propagation paths, *in* Geophysical prospecting: American Institute of Mining and Metallurgical Engineers Transactions, v. 97, p. 245-262.
- Farrow, R.A., 1976, Preliminary report on the geotechnical properties of the Wasatch Formation at Buffalo, Wyoming: U.S. Geological Survey Open-File Report 76-877, 76 p.
- 1980, Preliminary report on the geotechnical properties of the Fort Union Formation at Sheridan, Wyoming: U.S. Geological Survey Open-File Report 80-1246, 175 p.
- Gallagher, C.P., Henshaw, A.C., Money, M.S., and Tarling, D.H., 1978, The location of abandoned mine shafts in rural and urban environments: Bulletin of the International Association of Engineering Geology, no. 18, p. 179-185.
- Hasbrouck, W.P., and Hadsell, F.A., 1976, Geophysical exploration techniques applied to Western United States coal deposits, *in* Coal Exploration: International Coal Exploration Symposium, 1st, London, England, 1976, Proceedings, p. 256-287.
- Henshaw, A.C., 1977, The location of abandoned mine shafts using a proton magnetometer: University of Newcastle upon Tyne M.Sc. dissertation, p. 82.
- Keller, G.V., and Frischknecht, F.C., 1970, Electrical methods in geophysical prospecting: New York, Pergamon Press, p. 278-353.
- Kuzara, S.A., 1977, Black diamonds of Sheridan—a facet of Wyoming history: Cheyenne, Wyo., 1st ed., September, Pioneer Printing and Stationery Co., 125 p.
- Laby, T.H., 1931, The principles and practice of geophysical prospecting: Cambridge, England, Imperial Geophysical Survey Report, p. 337-341.
- Mapel, W.J., 1959, Geology and coal resources of the Buffalo-Lake De Smet area, Johnson and Sheridan Counties, Wyoming: U.S. Geological Survey Bulletin 1078, 148 p.
- Miller, C.H., 1979, Seismic, magnetic and geotechnical properties of a landslide and clinker deposits, Powder River Basin, Wyoming and Montana: U.S. Geological Survey Open-File Report 79-952, 47 p.
- Palmer, D., 1983, Comment on "Curved-ray path interpretation of seismic refraction data," by S. A. Greenhalgh and D. W. King: Geophysical Prospecting [Blackwell Scientific Publications Ltd., P.O. Box 88, Oxford, England], v. 31, no. 3, p. 542-543.
- Parasnis, D.S., 1966, Mining geophysics, Ser. 3 of Methods in geochemistry and geophysics: New York, Elsevier, 356 p.
- Redpath, B.B., 1973, Seismic refraction for engineering site investigations: U.S. Army Corps of Engineers Waterways Experiment Station, Explosive Excavation Research Laboratory, Livermore, Calif., 55 p.
- Rogers, G.S., 1917, Baked shale and slag formed by the burning of coal beds: U.S. Geological Survey Professional Paper 108, 10 p.
- Sheridan-Wyoming Coal Company, 1938, Coal mine map of the Acme Mine—Map of mine no. 42: U.S. Bureau of Mines, Building 20, Denver Federal Center, Denver, Colorado.
- Sheriff, R.E., 1974, Encyclopedic dictionary of exploration geophysics: Society of Exploration Geophysicists, 266 p.
- U.S. Army, 1977, Symposium on detection of subsurface cavities, Vicksburg, Mississippi, July 12-15, 1977: U.S. Army Chief of Engineers, U.S. Army Engineer Waterways Experiment Station, Soils and Pavements Laboratory, 191 p.
- 1981, Symposium on tunnel detection: U.S. Army Mobility Equipment Research and Development Command and Colorado School of Mines, Geophysics Department, Golden, CO 80401, 142 p.
- Watts, R.D., 1978, Electromagnetic scattering from buried wires: Geophysics, v. 43, no. 4, p. 767-781.

